Inorganic Chemistry
Article

Inorg. Chem. **2010**, *49*, 4405–4419 **4405**
DOI: 10.1021/ic901751z

Five- and Six-Coordinate Adducts of Nitrosamines with Ferric Porphyrins: Structural Models for the Type II Interactions of Nitrosamines with Ferric Cytochrome P450

Nan Xu,[†] Lauren E. Goodrich,[‡] Nicolai Lehnert,*[,‡] Douglas R. Powell,[†] and George B. Richter-Addo*[,†]

[†]*Department of Chemistry and Biochemistry, University of Oklahoma, 620 Parrington Oval, Norman, Oklahoma 73019, and* [‡]*Department of Chemistry, University of Michigan, 930 North University Avenue, Ann Arbor, Michigan 48109*

Received September 2, 2009

Nitrosamines are well-known for their toxic and carcinogenic properties. The metabolic activation of nitrosamines occurs via interaction with the heme-containing cytochrome P450 enzymes. We report the preparation and structural characterization of a number of nitrosamine adducts of synthetic iron porphyrins. The reactions of the cations $[(por)Fe(THF)_2]ClO_4$ (por = TPP, TTP, OEP) with dialkylnitrosamines (R_2NNO; $R_2 = Me_2$, Et_2, (*cyclo*-$CH_2)_4$, (*cyclo*-$CH_2)_5$, $(PhCH_2)_2$) in toluene generate the six-coordinate high-spin ($S = 5/2$) $[(por)Fe(ONNR_2)_2]ClO_4$ compounds and a five-coordinate intermediate-spin ($S = 3/2$) $[(OEP)Fe(ONNMe_2)]ClO_4$ derivative in 57−72% yields (TPP = 5,10,15,20-tetraphenylporphyrinato dianion, TTP = 5,10,15,20-tetra-*p*-tolylporphyrinato dianion, OEP = 2,3,7,8,12,-13,17,18-octaethylporphyrinato dianion). The N−O and N−N vibrations of the coordinated nitrosamine groups in $[(por)Fe(ONNR_2)_2]ClO_4$ occur in the 1239−1271 cm^{-1} range. Three of the six-coordinate $[(por)Fe(ONNR_2)_2]ClO_4$ compounds and one five-coordinate $[(OEP)Fe(ONNMe_2)]ClO_4$ compound have been characterized by single crystal X-ray crystallography. All the nitrosamine ligands in these complexes bind to the ferric centers via a sole η^1-O binding mode. No arylnitrosamine adducts were obtained from the reactions of the precursor compounds $[(por)Fe(THF)_2]ClO_4$ with three arylnitrosamines (Ph_2NNO, Ph(Me)NNO, Ph(Et)NNO). However, prolonged exposure of $[(por)Fe(THF)_2]ClO_4$ to these arylnitrosamines resulted in the formation of the known five-coordinate (por)Fe(NO) derivatives. The latter (por)Fe(NO) compounds were obtained more readily by the reactions of the three arylnitrosamines with the four-coordinate $(por)Fe^{II}$ precursors.

Introduction

Nitrosamines ($R_2N-N{=}O$; R = alkyl, aryl) belong to the class of *N*-nitroso compounds. These include the simple dialkylnitrosamines such as dimethylnitrosamine and diethylnitrosamine, and elaborate examples such as nitrosoureas and nitrosonicotine.[1,2] Nitrosamines occur in a wide range of environments such as cigarette smoke, beer, saliva, and in rubber nipples for feeding bottles.[3,4] Endogenous sources of nitrosamines are generally from the in vivo nitrosation of amines in the acidic stomach,[5] or by the macrophage-assisted nitrosation of amines.[6−8]

Nitrosamines are generally considered to be carcinogenic. They require metabolic activation by the heme-containing enzyme cytochrome P450 in the liver, lung, or nasal tissues to exert their carcinogenic effects.[1,9−12] The interaction of nitrosamines with the active site of cytochrome P450 can occur via two main paths. Several years ago, Appel and coworkers demonstrated that nitrosamines bind to the active

*To whom correspondence should be addressed. E-mail: lehnertn@umich.edu (N.L.), grichteraddo@ou.edu (G.B.R.-A.).

(1) *Nitrosamines and Related N-Nitroso Compounds. Chemistry and Biochemistry*; Loeppky, R. N., Michejda, C. J., Eds.; American Chemical Society: Washington, D.C., 1994; Vol. *553*.
(2) *Nitrosamines: Toxicology and Microbiology*; Hill, M. J., Ed.; VCH Ellis Horwood Ltd.: Chichester, England, 1988.
(3) Lijinsky, W. *Chemistry and Biology of N-Nitroso Compounds*; Cambridge University Press: Cambridge, 1992.
(4) Tannenbaum, S. R.; Archer, M. C.; Wishnok, J. S.; Bishop, W. W. *J. Nat. Cancer Inst.* **1978**, *60*, 251–253.
(5) Lintas, C.; Clark, A.; Fox, J.; Tannenbaum, S. R.; Newberne, P. M. *Carcinogenesis* **1982**, *3*, 161–165.
(6) Iyengar, R.; Stuehr, D. J.; Marletta, M. A. *Proc. Natl. Acad. Sci., U.S.A.* **1987**, *84*, 6369–6373.
(7) Wu, Y. N.; Brouet, I.; Calmels, S.; Bartsch, H.; Ohshima, H. *Carcinogenesis* **1993**, *14*, 7–10.
(8) Ohshima, H.; Tsuda, M.; Adachi, H.; Ogura, T.; Sugimura, T.; Esumi, H. *Carcinogenesis* **1991**, *12*, 1217–1220.
(9) *Human Cytochrome P450 Enzymes*, 3rd ed.; Guengerich, F. P., Ed.; Kluwer Academic/Plenum: New York, 2005.
(10) Yang, C. S.; Smith, T. J. *Adv. Exp. Med. Biol.* **1996**, *387*, 385–394.
(11) Ioannides, C.; Gibson, G. G. In *Safety Evaluation of Nitrosatable Drugs and Chemicals*; Gibson, G. G., Ioannides, C., Eds.; Taylor and Francis: London, 1981; pp 257−278.
(12) Hecht, S. S. *Chem. Res. Toxicol.* **1998**, *11*, 559–603.

Published on Web 04/14/2010

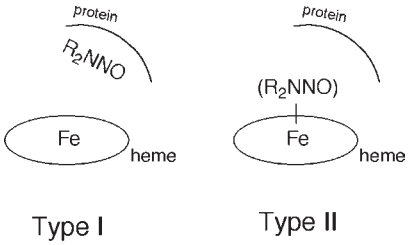

Figure 1. Type I and Type II interactions of nitrosamines with the active site of cytochrome P450.

site of cytochrome P450 through both Type I and Type II mechanisms as shown in Figure 1.[13]

The Type I interaction is typical of cytochrome P450 monooxygenase systems in their interaction with substrates, where the nitrosamine binds to the protein pocket site near the iron center in preparation for its α-hydroxylation and subsequent chemical modification to generate highly reactive organic species. The Type II interaction places the nitrosamine in direct contact with the iron center in cytochrome P450. Despite this important observation by Appel and co-workers, very little is known about the Type II heme-nitrosamine interaction.

The reactions of dialkylnitrosamines with synthetic iron and manganese porphyrins in the presence of oxidants have yielded decomposition products such as the aldehydes, presumably via initial α-hydroxylation of the nitrosamine.[14,15] Interestingly, exposure of phenobarbital-treated mouse liver to diethylnitrosamine resulted in the formation of the *N*-alkylated green pigment *N*-hydroxyethylprotoporphyrin IX.[16]

Nitrosamines have been shown to bind to metal centers via one of four binding modes as illustrated in Figure 2.

The binding mode **A** was the first to be established by X-ray crystallography in 1968, and this was for a copper complex oligomer of the form $\{(Me_2NNO)CuCl_2\}_n$.[17,18] The binding mode **B** was established in 1980 for a Pd complex of the form $Pd\{N(O)N(Me)C_6H_4\}Cl(PPh_3)$.[19] Although binding mode **C** had been proposed for a series of Lewis acid adducts of nitrosamines (based on IR and ^{1}H NMR spectroscopy),[20] no metal-nitrosamine complex with this binding mode was reported until our preparation and crystallization in 1995 of a diethylnitrosamine adduct of a ferric porphyrin, namely, $[(TPP)Fe(ONNEt_2)_2]ClO_4$ (TPP = tetraphenylporphyrinato dianion).[21,22] Recently, Doctorovich and co-workers have confirmed the binding mode **D** (Figure 2) that results

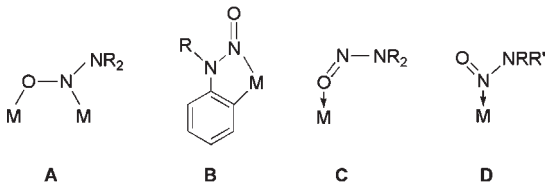

Figure 2. Crystallographically determined binding modes of nitrosamines to metal centers.

from nucleophilic attack of primary amines on the coordinated nitrosyl ligand in $K[IrCl_5NO]$.[23,24]

To further probe the interactions of nitrosamines with heme, we embarked on a systematic study of the reactions of nitrosamines with both ferric and ferrous porphyrins, with the goal of establishing the conditions that are suitable for simple adduct formation of the Type II class and the conditions that promote denitrosation of the nitrosamines. In this article, we report the successful preparation, isolation, and crystallographic characterization of non-cyclic and cyclic dialkylnitrosamine adducts of ferric porphyrins. We show that both six-coordinate and five-coordinate complexes can be obtained. This allows, for the first time, for a comparison between the geometric parameters of bound dialkylnitrosamines to ferric porphyrins as a function of nitrosamine alkyl substitution, and a comparison of the reactivity of dialkyl and aryl nitrosamines with iron porphyrins. In addition, low-temperature electron paramagnetic resonance (EPR) spectroscopy has been employed on solid state and frozen solution samples to ascertain the spin states of these ferric nitrosamine complexes. To the best of our knowledge, these compounds, together with our previously reported $[(TPP)Fe(ONNEt_2)_2]^+$ compound,[21,22] represent the only structural models of the Type II interactions between nitrosamines and heme known to date.

Experimental Section

All reactions were performed under an atmosphere of prepurified nitrogen using standard Schlenk glassware and/or in an Innovative Technology Labmaster 100 Drybox. Solutions for spectral studies were also prepared under a nitrogen atmosphere. Solvents were distilled from appropriate drying agents under nitrogen just prior to use: CH_2Cl_2 (CaH_2), hexane (CaH_2), toluene (Na).

Chemicals. *N*-nitrosodimethylamine (Me_2NNO, 99%), *N*-nitrosodiethylamine (Et_2NNO, >99%), *N*-nitrosodiphenylamine (Ph_2NNO, >97.0%), $AgClO_4$ (97%), were purchased from Aldrich Chemical Co. and used as received. *N*-nitrosopiperidine ((*cyclo*-$CH_2)_5NNO$, 99%) and *N*-nitrosopyrrolidine ((*cyclo*-$CH_2)_4NNO$, 99%) were purchased from Fluka. $[(TPP)Fe^{III}(THF)_2]ClO_4$[22] and *N*-nitrosodibenzylamine ($(PhCH_2)_2NNO$[25] were prepared by published procedures. *N*-ethyl-*N*-nitrosoaniline (Ph(Et)NNO), *N*-methyl-*N*-nitrosoaniline (Ph(Me)NNO) and the nitroso ^{15}N-labeled compounds $Et_2N^{15}NO$, (*cyclo*-$CH_2)_4N^{15}NO$ and $(PhCH_2)_2N^{15}NO$ were prepared in a manner similar to that used to prepare the unlabeled $(PhCH_2)_2NNO$,[25] but using $Na^{15}NO_2$ instead of $NaNO_2$ in the nitrosation reactions. Nitric oxide (98%, Matheson Gas) was passed through KOH pellets and a cold trap (dry ice/acetone) to remove higher nitrogen oxides.

Caution! *Nitrosamines (R_2NNO) are generally considered to be toxic; thus, they were handled with extreme care in a Drybox or in*

(13) Appel, K. E.; Ruf, H. H.; Mahr, B.; Schwarz, M.; Rickart, R.; Kunz, W. *Chem.-Biol. Interact*. **1979**, *28*, 17–33.
(14) Mochizuki, M.; Okochi, E.; Shimoda, K.; Ito, K. In *Nitrosamines and Related N-Nitroso Compounds*; Loeppky, R. N., Michejda, C. J., Eds.; American Chemical Society: Washington, D.C., 1994; Chapter 113, pp 158−168.
(15) Okochi, E.; Mochizuki, M. *Chem. Pharm. Bull*. **1995**, *43*, 2173–2176.
(16) White, I. N. H.; Smith, A. G.; Farmer, P. B. *Biochem. J*. **1983**, *212*, 599–608.
(17) Klement, U. *Acta Crystallogr*. **1969**, *B25*, 2460–2465.
(18) Klement, U.; Schmidpeter, A. *Angew. Chem., Int. Ed. Engl*. **1968**, *7*, 470.
(19) Constable, A. G.; McDonald, W. S.; Shaw, B. L. *J. Chem. Soc., Dalton Trans*. **1980**, 2282–2287.
(20) Schmidpeter, A. *Chem. Ber*. **1963**, *96*, 3275–3279.
(21) Yi, G.-B.; Khan, M. A.; Richter-Addo, G. B. *J. Am. Chem. Soc*. **1995**, *117*, 7850–7851.
(22) Chen, L.; Yi, G.-B.; Wang, L.-S.; Dharmawardana, U. R.; Dart, A. C.; Khan, M. A.; Richter-Addo, G. B. *Inorg. Chem*. **1998**, *37*, 4677–4688.
(23) Doctorovich, F.; Di Salvo, F.; Escola, N.; Trapani, C.; Shimon, L. *Organometallics* **2005**, *24*, 4707–4709.
(24) Di Salvo, F.; Estrin, D. A.; Leitus, G.; Doctorovich, F. *Organometallics* **2008**, *27*, 1985–1995.
(25) Zolfigol, M. A. *Synth. Commun*. **1999**, *29*, 905–910.

Schlenk glassware to minimize exposure to either the vapor or the material. Detailed procedures for the disposal of carcinogenic nitrosamines have been published.[26] *Because of potential explosion and fire hazards, the perchlorate compounds were prepared in small amounts and handled carefully.*

Instrumentation. Infrared spectra were recorded on a Bio-Rad FT-155 FTIR spectrometer. EPR spectra were recorded on a Bruker X-band EMX spectrometer equipped with an Oxford Instruments liquid helium cryostat. The solution EPR spectra were obtained on ~2 mM frozen toluene solutions using ~20 mW microwave power and 100 kHz field modulation with the amplitude set to 1 G. EPR spectra were simulated using the program SpinCount (version 2.2.40) written by Prof. Michael Hendrich, Carnegie Mellon University. This program uses the following Spin Hamiltonian to describe exchange interactions: $\underline{H} = J_{AB} \cdot \underline{S}_A \cdot \underline{S}_B$; i.e., $J > 0$ implies antiferromagnetic coupling.

Preparation of [(TPP)Fe(ONNMe$_2$)$_2$]ClO$_4$. To a toluene solution (20 mL) of [(TPP)Fe(THF)$_2$]ClO$_4$ (0.042 g, 0.048 mmol) was added Me_2NNO (0.11 mL, 1.5 mmol). The mixture was stirred for 45 min, during which time the color of the solution changed from brown-purple to red-purple. The solvent was reduced to ~10 mL, and hexane (30 mL) was added. The resulting solution was placed in a freezer (−22 °C) overnight. The violet crystalline solid that formed was collected by filtration, washed with hexane (2 × 15 mL), and dried in vacuo to give [(TPP)Fe(ONNMe$_2$)$_2$]ClO$_4$ (0.029 g, 0.032 mmol, 66% isolated yield). Slow evaporation of a CH_2Cl_2/hexane (3:1 ratio; 5 mL) solution of the product at room temperature gave suitable crystals for X-ray diffraction studies. Anal. Calcd for $C_{48}H_{36}O_6N_8ClFe \cdot 0.05CH_2Cl_2 \cdot 0.6C_6H_{14}$: C, 64.08; H, 4.63; N, 11.57; Cl, 4.03. Found: C, 62.55; H, 4.30; N, 11.23; Cl, 3.91. IR (KBr, cm^{-1}): $\upsilon_{NO/NN}$ 1256 m; also υ_{ClO_4} 1119 m, 1102 s, 1073 m, 1061 w, 623 m.

The other bis-nitrosamine complexes were generated similarly using the respective porphyrin macrocycles and nitrosamines (TTP = tetratolylporphyrinato dianion):

[(TTP)Fe(ONNMe$_2$)$_2$]ClO$_4$. Yield: 60%. IR (KBr, cm^{-1}): $\upsilon_{NO/NN}$ 1255 m; also υ_{ClO_4} 1117 m, 1101 s, 1073 m, 1062 m, 623 m.

[(TPP)Fe(ONNEt$_2$)$_2$]ClO$_4$. This compound was prepared as previously described in reference 22. IR (NaCl, cm^{-1}): $\upsilon_{NO/NN}$ 1271 m; also υ_{ClO_4} 1098 s, 1074 m, 623 m.

[(TPP)Fe(O^{15}NNEt$_2$)$_2$]ClO$_4$. IR (NaCl, cm^{-1}): $\upsilon_{^{15}NO/N^{15}N}$ 1252 m.

[(TTP)Fe(ONNEt$_2$)$_2$]ClO$_4$. Yield: 66%. IR (KBr, cm^{-1}): $\upsilon_{NO/NN}$ 1267 m; also υ_{ClO_4} 1136 m, 1122 m, 1109 s, 1091 s, 626 m.

[(TPP)Fe(ONN(CH$_2$Ph)$_2$)$_2$]ClO$_4$. Yield: 61%. IR (KBr, cm^{-1}): $\upsilon_{NO/NN}$ 1268 m; also υ_{ClO_4} 1125 m, 1096 s, 1073 m, 624 m. Slow evaporation of a CH_2Cl_2/hexane (3:1 ratio) solution of the product generated suitable crystals of the mixed salt [(TPP)Fe(ONN(CH$_2$Ph)$_2$)$_2$][(TPP)Fe(ClO$_4$)$_2$] for X-ray diffraction studies.

[(TPP)Fe(O^{15}NN(CH$_2$Ph)$_2$)$_2$]ClO$_4$. IR (KBr, cm^{-1}): $\upsilon_{^{15}NO/N^{15}N}$ 1254 m.

[(TPP)Fe(ONN(*cyclo*-CH$_2$)$_4$)$_2$]ClO$_4$. Yield: 72%. IR (KBr, cm^{-1}): $\upsilon_{NO/NN}$ 1239 m; also υ_{ClO_4} 1093 s br, 1075 m, 622 m.

[(TPP)Fe(ONN(*cyclo*-CH$_2$)$_5$)$_2$]ClO$_4$. Yield: 57%. Suitable crystals for X-ray diffraction studies were grown at room temperature by slow evaporation of a solution of the product in CH_2Cl_2/hexane (3:1 ratio). IR (KBr, cm^{-1}): $\upsilon_{NO/NN}$ 1242 s; also υ_{ClO_4} 1122 w, 1096 s br, 1071 m, 623 m.

[(TPP)Fe(O^{15}NN(*cyclo*-CH$_2$)$_5$)$_2$]ClO$_4$. IR (KBr, cm^{-1}): $\upsilon_{^{15}NO/N^{15}N}$ 1225 m.

Preparation of the Five-Coordinate [(OEP)Fe(ONNMe$_2$)]ClO$_4$. This compound was generated in a manner similar to that used to prepare the six-coordinate compound [(TPP)Fe(ONNMe$_2$)$_2$]ClO$_4$ except that the OEP macrocycle was used in place of TPP. Yield: 68%. Anal. Calcd for $C_{38}H_{50}O_5N_6ClFe \cdot 0.1CH_2Cl_2 \cdot 0.5C_6H_{14}$: C, 60.67; H, 7.08; N, 10.33; Cl, 5.23. Found: C, 59.42; H, 6.57; N, 10.48; Cl, 4.84. IR (KBr, cm^{-1}): $\upsilon_{NO/NN}$ 1239 m, υ_{ClO_4} 1091 br, 623 s.

Preparation of [(TPP)Fe(NO)(ONNMe$_2$)]ClO$_4$. Method I. Nitric oxide was bubbled through a CH_2Cl_2 solution (15 mL) of [(TPP)Fe(ONNMe$_2$)$_2$]ClO$_4$ (50 mg, 0.055 mmol) for 2 min. During this time, the color of the mixture changed from red-purple to bright-red. The volume of solution was reduced to ~5 mL, and hexane (20 mL) was added. A dark purple crystalline solid formed after ~30 min. The solid was collected by filtration, washed with hexane (2 × 15 mL), and dried in vacuo to give the bright red [(TPP)Fe(NO)(ONNMe$_2$)]ClO$_4$ (0.023 g, 0.028 mmol, 56% isolated yield). IR (NaCl, cm^{-1}): υ_{NO} 1922 m, $\upsilon_{NO/NN}$ 1245 m, υ_{ClO_4} 1098 s, 1074 m, 620 s.

Method II. Crystals of [(TPP)Fe(ONNMe$_2$)$_2$]ClO$_4$ in a vial under an N_2 atmosphere were exposed to NO gas for 5 h. The vial was then purged with N_2 to remove unreacted NO. An IR spectroscopic analysis of the product identified it as the bright red crystalline [(TPP)Fe(NO)(ONNMe$_2$)]ClO$_4$. IR (KBr, cm^{-1}): υ_{NO} 1910 m, $\upsilon_{NO/NN}$ 1253 m; also, υ_{ClO_4} 1117 m, 1101 s, 1072 m, 1061 w, 623 m. The crystals obtained under these conditions, unfortunately, did not diffract X-rays.

Preparation of [(TPP)Fe(NO)(ONNEt$_2$)]ClO$_4$. This compound was prepared as described previously in reference 22 (i.e., by Method I above). Yield: 39%. IR (NaCl, cm^{-1}): υ_{NO} 1923 m, $\upsilon_{NO/NN}$ 1267 m; also υ_{ClO_4} 1096 s, 1075 m, 622 m.

[(TPP)Fe(NO)(O^{15}NNEt$_2$)]ClO$_4$.. IR (NaCl, cm^{-1}): υ_{NO} 1924 m, $\upsilon_{^{15}NO/N^{15}N}$ 1248 m.

Reaction of Ferrous (TPP)Fe^{II} with Ph$_2$NNO. The four-coordinate compound (TPP)Fe^{II} (0.090 mg, 0.135 mmol) was prepared in situ by the reduction of equimolar (TPP)FeCl in CH_2Cl_2 by Zn amalgam. The solution was filtered into a Schlenk tube, and solid Ph_2NNO (0.029 g, 0.145 mmol) was added to the stirred solution. The mixture was stirred for an additional 10 min during which time the color of the solution changed from red to dark red. The solvent was reduced to ~5 mL and hexane (30 mL) was added, and the solution placed in a freezer (−22 °C) overnight. The resulting dark red solid was collected by filtration and dried in vacuo to give the known five-coordinate compound (TPP)Fe(NO) (0.036 g, 0.052 mmol, 38% isolated yield). IR (KBr, cm^{-1}): υ_{NO} 1701 m.

A similar reaction using either of the two *monoaryl* nitrosamines Ph(Me)NNO or Ph(Et)NNO resulted in the generation of (TPP)Fe(NO) in lower yields (estimated ~1/4 of that from the Ph_2NNO reaction, as judged by IR spectroscopy).

Solid-State Structural Determinations. Details of crystal data and refinement are given in Table 1. Single-crystal X-ray diffraction data were collected using an instrument with a Bruker APEX ccd area detector with graphite-monochromated Mo Kα radiation (λ = 0.71073 Å). The structures were solved by direct methods using the SHELXTL system and refined by full-matrix least-squares methods on F^2.

(i). [(OEP)Fe(ONNMe$_2$)]ClO$_4$·CH$_2$Cl$_2$. Cell parameters were determined from a non-linear least-squares fit of 5660 peaks in the range $2.21 < \theta < 28.29°$. A total of 28480 data were measured in the range $1.60 < \theta < 28.30°$ using ω oscillation frames. The data were merged to form a set of 10055 independent data with R(int) = 0.0443 and a coverage of 100.0%. The triclinic space group $P\bar{1}$ was determined by statistical tests and verified by subsequent refinement. Non-hydrogen atoms were refined with anisotropic displacement parameters. Hydrogen atom positions were initially determined by geometry and refined by a riding model; hydrogen atom displacement parameters were set to 1.2× (1.5× for methyl) the displacement parameters of the bonded atoms. A total of 525 parameters were refined against 36 restraints and 10055 data to give $wR(F^2)$ = 0.1298 and S = 1.001 for

(26) Lunn, G.; Sansone, E. B.; Keefer, L. K. *Carcinogenesis* **1983**, *4*, 315–319.

Table 1. Crystal Data and Structure Refinement

compound	[(OEP)Fe(ONNMe$_2$)]ClO$_4$[a]	[(TPP)Fe(ONNMe$_2$)$_2$]ClO$_4$	[(TPP)Fe(ONN(CH$_2$Ph)$_2$)$_2$]-[(TPP)Fe(ClO$_4$)$_2$] [b]	[(TPP)Fe(ONN(*cyclo*-CH$_2$)$_5$)$_2$]ClO$_4$[b]
formula (f.w.)	(C$_{38}$H$_{50}$FeN$_6$O$_5$Cl$_1$)·(CH$_2$Cl$_2$) (847.07)	C$_{48}$H$_{40}$ClFeN$_8$O$_6$ (915.21)	(C$_{116}$H$_{84}$Fe$_2$N$_{12}$O$_{10}$Cl$_2$)·(CH$_2$Cl$_2$)$_2$ (2158.40)	(C$_{54}$H$_{48}$Cl$_1$FeN$_8$O$_6$)·(CH$_2$Cl$_2$)$_2$ (1166.16)
T (K)	100(2)	103(2)	97(2)	113(2)
crystal system	Triclinic	Monoclinic	Triclinic	Triclinic
space group	$P\bar{1}$	$C2/c$	$P\bar{1}$	$P\bar{1}$
a (Å), α (deg)	12.441(2), 64.645(6)	17.535(2), 90	12.3159(14), 100.690(5)	12.0211(12), 113.7120(10)
b (Å), β (deg)	13.634(3), 66.076(6)	17.625(2), 119.315(2)	13.7776(16), 107.620(5)	14.7595(14), 96.7340(10)
c (Å), γ (deg)	14.814(3), 69.444(7)	15.7926(18), 90	16.972(2), 107.860(5)	17.9330(17), 104.3430(10)
V, Z/Z'	2027.2(7), 2/1	4255.8(8) Å^3, 4	2486.5(5) Å^3, 1/0.5	2736.7(5), 2
D(calcd), g/cm^3	1.388	1.430	1.441	1.415
abs coeff, mm^{-1}	0.620	0.479	0.524	0.578
F(000)	890	1900	1114	1206
crystal size (mm)	0.40 × 0.31 × 0.17	0.26 × 0.16 × 0.12	0.74 × 0.38 × 0.19	0.50 × 0.31 × 0.17
θ range for data collection	1.60−28.30°	1.76−28.29°	1.84−26.00°	1.53−27.50°
index ranges	$-16 \le h \le 16$ $-18 \le k \le 18$ $-19 \le l \le 19$	$-23 \le h \le 22$ $-23 \le k \le 22$ $-20 \le l \le 20$	$-15 \le h \le 15$ $-16 \le k \le 16$ $-20 \le l \le 20$	$-15 \le h \le 15$ $-19 \le k \le 19$ $-23 \le l \le 23$
reflections collected	28480	25807	27426	33328
independent reflns	10055 [R_{int} = 0.0443]	5153 [R_{int} = 0.0281]	9718 [R_{int} = 0.0149]	12423 [R_{int} = 0.0176]
max. and min transmission	0.984 and 0.787	0.9448 and 0.8856	0.9071 and 0.6979	0.9081 and 0.7610
data/restraints/parameters	10055/36/525	5153/0/293	9718/0/670	12423/0/688
goodness-of-fit on F^2	1.001	1.034	1.004	1.032
final R indices [$I > 2\sigma(I)$]	R1 = 0.0488	R1 = 0.0334	R1 = 0.0299	R1 = 0.0431
R indices (all data)	wR2 = 0.1298	wR2 = 0.0898	wR2 = 0.0845	wR2 = 0.1189
largest diff. peak and hole, e Å^{-3}	0.716 and −0.554	0.485 and −0.382	0.342 and −0.502	0.942 and −0.896

[a] This compound crystallizes as a dichloromethane solvate. [b] These two complexes crystallize as bis-dichloromethane solvates.

weights of $w = 1/[\sigma^2(F^2) + (0.0620P)^2 + 1.4200P]$, where $P = [F_o^2 + 2F_c^2]/3$. The final $R(F)$ was 0.0488 for the 8001 observed, $[F > 4\sigma(F)]$, data. The largest shift/s.u. was 0.001 in the final refinement cycle.

(ii). [(TPP)Fe(ONNMe$_2$)$_2$]ClO$_4$. Intensity data, which covered approximately the full sphere of the reciprocal space, were measured as a series of ω oscillation frames each spanning 0.3° for 25 s/frame. Coverage of unique data was 97.3% complete to 56.6°(2θ). Cell parameters were determined from a non-linear least-squares fit of 6877 reflections in the range $2.3 < \theta < 28.3$. All the non-hydrogen atoms were refined anisotropically, and all the hydrogen atoms were included with idealized parameters. The asymmetric unit contains half of the C$_{48}$H$_{40}$N$_8$O$_2$Fe cation that sits around the crystallographic inversion center, and a perchlorate anion that sits on the crystallographic 2-fold center.

(iii). [(TPP)Fe(ONN(CH$_2$Ph)$_2$)$_2$][(TPP)Fe(ClO$_4$)$_2$]·(CH$_2$Cl$_2$)$_2$. Both the iron porphyrin cation and anion were located on crystallographic centers of symmetry. Cell parameters were determined from a non-linear least-squares fit of 8770 peaks in the range $2.48 < \theta < 28.27°$. A total of 27426 data were measured in the range $1.84 < \theta < 26.00°$ using ω oscillation frames. The data were merged to form a set of 9718 independent data with R(int) = 0.0149 and a coverage of 99.6%. The triclinic space group $P\bar{1}$ was determined by statistical tests and verified by subsequent refinement. Non-hydrogen atom were refined with anisotropic displacement parameters. Hydrogen atom positions were initially determined by geometry and refined by a riding model; hydrogen atom displacement parameters were set to 1.2× the displacement parameters of the bonded atoms. A total of 670 parameters were refined against 9718 data to give $wR(F^2) = 0.0845$ and $S = 1.004$ for weights of $w = 1/[\sigma^2(F^2) + (0.0500P)^2 + 1.4800P]$, where $P = [F_o^2 + 2F_c^2]/3$. The final $R(F)$ was 0.0299 for the 9320 observed, $[F > 4\sigma(F)]$, data. The largest shift/s.u. was 0.001 in the final refinement cycle.

(iv). [(TPP)Fe((*cyclo*-CH$_2$)$_5$NNO)$_2$]ClO$_4$·(CH$_2$Cl$_2$)$_2$. Intensity data, which approximately covered the full sphere of the reciprocal space, were measured as a series of two oscillation frames each 0.3° for 17 s/frame. Coverage of unique data was 98.6% complete to 55.0° (2θ). Cell parameters were determined from a non-linear least-squares fit of 8246 reflections in the range $2.6 < \theta < 28.3°$. Non-hydrogen atoms were refined anisotropically, and all hydrogen atoms were included with idealized parameters.

The crystallographic data for the complexes are summarized in Table 1.

Results and Discussion

Appel and co-workers have provided spectroscopic evidence for a direct interaction between carcinogenic nitrosamines and the ferric center of liver microsomal cytochrome P450.[13] This Type II interaction (Figure 1) complements the typical substrate-distal pocket Type I interaction characteristic of cytochrome P450-induced α-hydroxylation reactions. Despite this observation of a Type II interaction between nitrosamines and cytochrome P450, there is surprisingly little information regarding the direct interactions of nitrosamines with the metal center in iron porphyrins.

Several years ago, we reported the first such adduct between a nitrosamine and an iron porphyrin, namely, the ferric high-spin complex [(TPP)Fe(ONNEt)$_2$]ClO$_4$.[21,22] To date, this remains the only synthetic iron porphyrin nitrosamine compound in the literature. As part of our work to expand on our knowledge regarding the structural consequences of such interactions, we have prepared other ferric porphyrin nitrosamine compounds and determined their crystal structures.

The six-coordinate compounds were prepared by displacing coordinated solvent from the precursor compound.

$$[(\mathrm{por})\mathrm{Fe}(\mathrm{THF})_2]\mathrm{ClO_4} + \text{excess } \mathrm{R_2NNO} \rightarrow [(\mathrm{por})\mathrm{Fe}(\mathrm{ONNR_2})_2]\mathrm{ClO_4} + 2\mathrm{THF}$$
$$\mathrm{R_2} = \mathrm{Me_2}, \mathrm{Et_2}, (\mathrm{CH_2Ph})_2, (\textit{cyclo}\text{-}\mathrm{CH_2})_4, (\textit{cyclo}\text{-}\mathrm{CH_2})_5 \quad (1)$$

Thus, the reactions of [(por)Fe(THF)$_2$]ClO$_4$ (por = TPP, TTP) with five different nitrosamines (*N*-nitrosodimethylamine (Me$_2$NNO), *N*-nitrosodiethylamine (Et$_2$NNO),

Table 2. IR Data for ν_{NO} and ν_{NN} in Nitrosamine Iron Porphyrin Complexes and the Corresponding Uncomplexed Nitrosamines

compound	$\nu_{NO/NN}$ (cm^{-1})	ref
$[(OEP)Fe(ONNMe_2)]ClO_4$[a]	1239	this work
$[(TPP)Fe(ONNMe_2)_2]ClO_4$[a]	1256	this work
$[(TTP)Fe(ONNMe_2)_2]ClO_4$[a]	1255	this work
$[(TPP)Fe(ONNEt_2)_2]ClO_4$[b]	1271	this work[22]
$[(TPP)Fe(O^{15}NNEt_2)_2]ClO_4$[b]	1252	this work
$[(TTP)Fe(ONNEt_2)_2]ClO_4$[a]	1267	this work
$[(TPP)Fe(ONN(cyclo\text{-}CH_2)_4)_2]ClO_4$[a]	1239	this work
$[(TPP)Fe(ONN(cyclo\text{-}CH_2)_5)_2]ClO_4$[a]	1242	this work
$[(TPP)Fe(O^{15}NN(cyclo\text{-}CH_2)_5)_2]ClO_4$[a]	1225	this work
$[(TPP)Fe(ONN(CH_2Ph)_2)_2]ClO_4$[a]	1268	this work
$[(TPP)Fe(O^{15}NN(CH_2Ph)_2)_2]ClO_4$[a]	1254	this work

free nitrosamines[c]	ν_{NO} (cm^{-1})	ν_{NN} (cm^{-1})	ref
Me_2NNO	1460	1035	27
Et_2NNO	1454	1060	27
$(cyclo\text{-}CH_2)_4NNO$	1428	1154	27
$(cyclo\text{-}CH_2)_5NNO$	1437	1087	27
$(PhCH_2)_2NNO$	1463	1120	27

[a] IR spectra were recorded as KBr pellets. [b] IR spectra were recorded as dried samples on NaCl discs. [c] IR spectra were recorded as CCl_4 solutions.

N-nitrosodibenzylamine ($(PhCH_2)_2NNO$), *N*-nitrosopyrrolidine ($(cyclo\text{-}CH_2)_4NNO$), and *N*-nitrosopiperidine ($(cyclo\text{-}CH_2)_5NNO$)) in toluene generate, after workup, the dark purple products in 57−72% isolated yields. The nitrosamine ligands dissociate readily from the iron center in these compounds, and we find that the use of excess nitrosamine assures reasonable yields of the products. In addition, we find that these products convert in solution to the ferric bis-aquo derivatives and the ferric μ-oxo dimer (i.e., $[(por)Fe]_2(\mu\text{-}O)$) in the presence of moisture and laboratory air/oxygen, respectively. The mechanism of decomposition of the bis-nitrosamine complexes to the μ-oxo dimer is unknown. In the solid state, however, these bis-nitrosamine compounds are fairly air-stable.

The IR spectra of the six-coordinate ferric $[(por)Fe(ONNR_2)_2]^+$ complexes as KBr pellets (or as dried samples on NaCl disks) show either one or two new bands in the 1200−1300 cm^{-1} region that could be associated with the ν_{NO} and ν_{NN} for the coordinated nitrosamines. However, nitrosamine ^{15}N-labeling reveals that only one of these is associated with the coordinated nitrosamines (Table 2 and Supporting Information), suggesting an overlap of the ν_{NO} and ν_{NN} bands in these complexes. For example, the IR spectrum of $[(TPP)Fe(ONNEt_2)_2]ClO_4$ shows a new band at 1271 cm^{-1} (absent in the precursor complex $[(TPP)Fe(THF)_2]ClO_4$) that shifts to 1252 cm^{-1} upon ^{15}N-labeling of the nitrosamine (Figure 3). Similar ^{15}N shifts in the IR spectra are observed upon isotopic labeling of the nitrosamines in the complexes $[(TPP)Fe(ONN(cyclo\text{-}CH_2)_5)_2]ClO_4$ (Δ = 14 cm^{-1}) and $[(TPP)Fe(ONN(CH_2Ph)_2)_2]ClO_4$ (Δ = 17 cm^{-1}) (Supporting Information).

We note that the uncomplexed aliphatic secondary nitrosamines used in this study display ν_{NO} and ν_{NN} bands in the 1428−1463 and 1035−1154 cm^{-1} ranges, respectively, in CCl_4.[27] Thus, the observed ν_{NO}s in the ferric porphyrin nitrosamine adducts are lower (i.e., weaker N−O bond) than those of the free nitrosamines, and the corresponding ν_{NN}s are higher (i.e., stronger N−N bond); this suggests that the coordinated

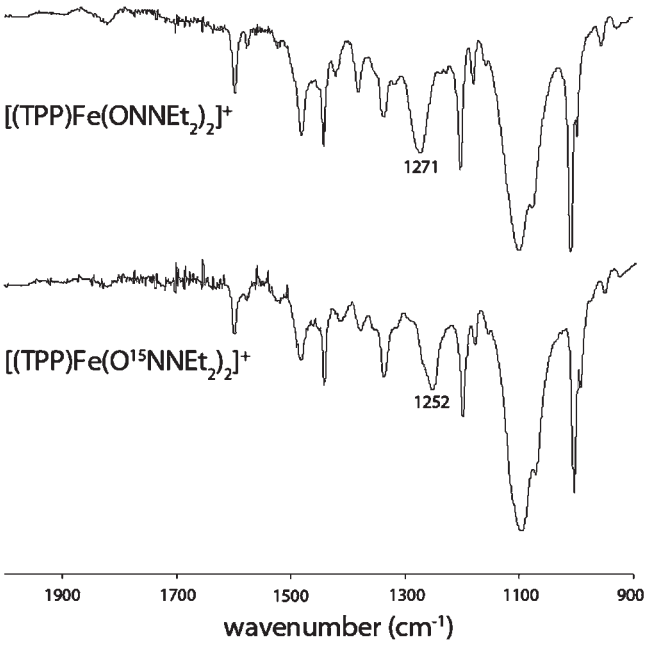

Figure 3. IR spectra of the unlabeled (top) and nitroso ^{15}N-labeled (bottom) diethylnitrosamine complex $[(TPP)Fe(ONNEt_2)_2]ClO_4$ as dried samples on NaCl plates.

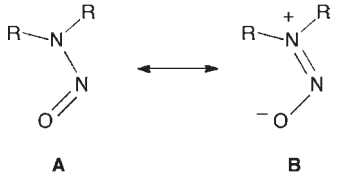

Figure 4. Dipolar resonance contributions of nitrosamines.

nitrosamines are best represented by a resonance hybrid having a significant contribution from structure **B** in Figure 4.

Unlike the case for the free nitrosamines, the ν_{NO} and ν_{NN} bands are coincident in the six-coordinate iron porphyrin nitrosamine compounds (Table 2). For these $[(por)Fe(ONNR_2)_2]ClO_4$ compounds, bands centered at ~1100 (br) and ~622 cm^{-1} were also observed for the υ_3 and υ_4 vibrations of the uncoordinated perchlorate anion.[28]

Because of the weak binding of the nitrosamine ligands to the ferric center in these six-coordinate compounds, as evidenced by ready displacement of these ligands by water (moisture), we reasoned that we might be able to take advantage of the stabilization energy provided by the $\pi-\pi$ porphyrin stacking observed in some OEP-type compounds to prepare a five-coordinate nitrosamine compound. This turned out to be the case, and we successfully prepared the mononitrosamine compound $[(OEP)Fe(ONNMe_2)]ClO_4$ and determined its crystal structure (see later).

Arylnitrosamines and Ferric Porphyrins. We attempted to prepare the analogous arylnitrosamine adducts by reacting the precursor compound $[(TPP)Fe(THF)_2]ClO_4$ with three aryl nitrosamines Ph(Me)NNO, Ph(Et)NNO, and Ph_2NNO. We were unsuccessful at detecting or isolating the expected nitrosamine adducts. It is likely that the electron-withdrawing phenyl group(s) in these

(27) Williams, R. L.; Pace, R. J.; Jeacocke, G. J. *Spectrochim. Acta* **1964**, *20*, 225–236.

(28) Gowda, N. M. N.; Naikar, S. B.; Reddy, G. K. N. *Adv. Inorg. Chem.* **1984**, *28*, 255–299.

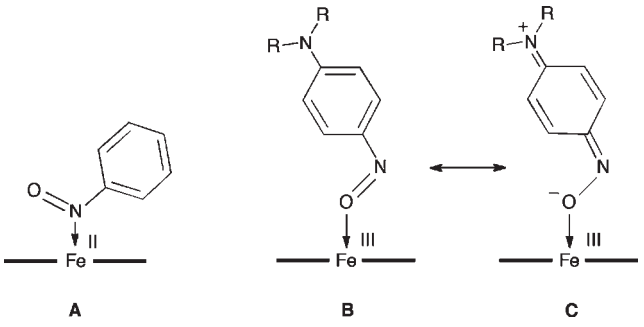

Figure 5. *N*-binding and *O*-binding modes of nitrosoarenes to iron porphyrins.

nitrosamines disfavor the dipolar resonance contribution (**B** in Figure 4) thus also disfavoring the partially negative charge on the nitrosamine O atom needed for coordination to the cationic "hard" ferric ion. We did find, however, that prolonged exposure of the $[(TPP)Fe(THF)_2]ClO_4$ compound to these nitrosamines (e.g., for 2 d) resulted in the formation of the known five-coordinate (TPP)Fe(NO) compound. Arylnitrosamines are known to act as NO donors.[29,30] Subsequent reduction of the cationic ferric center by NO is likely responsible for this reductive nitrosylation process to give the (TPP)Fe(NO) product.[31]

Nitrosamines and Ferrous Porphyrins. Expanding on the work by Mansuy and co-workers,[32] we have shown that nitrosoalkanes bind to ferrous porphyrins via the N atoms of the *C*-nitroso functionalities to give Fe{N(=O)R} moieties.[33] In the case of nitrosoarenes, we also demonstrated *N*-binding of the nitroso moiety to the ferrous center (**A** in Figure 5).[34] However, the hitherto unprecedented *O*-binding mode of the nitrosoarene was evident in its binding to ferric porphyrins if the ArNO ligand was appropriately *para*-substituted to enable a contribution of a dipolar resonance form (**B** and **C** in Figure 5).[34]

The *O*-binding modes in structures **B** and **C** in Figure 5 are analogous to those observed in our ferric nitrosamine complexes. We thus sought to prepare ferrous porphyrin complexes displaying the analogous *N*-bonded nitrosamine binding modes (Figure 6) from the reaction of nitrosamines with ferrous porphyrins.

The room temperature reactions of the aliphatic nitrosamines with the ferrous (por)Fe^{II} complexes did not, at least in our hands, form isolable adducts or other products. On the other hand, the room temperature reactions of the three arylnitrosamines with the (por)Fe^{II} compounds produced the known five-coordinate nitrosyl (por)Fe(NO) derivatives. For example, the reaction of (TPP)Fe^{II} with Ph_2NNO in CH_2Cl_2 produced (TPP)Fe(NO) in ~38% isolated yield (eq 2).

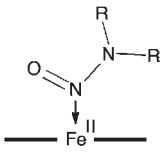

Figure 6. Proposed *N*-binding of nitrosamines to ferrous porphyrins.

$$(TPP)Fe + Ph_2NNO \rightarrow (TPP)Fe(NO) \qquad (2)$$

The denitrosation reactions involving the monoaryl nitrosamines generally took longer to generate the (por)Fe(NO) products. The N−N bond in aromatic *N*-nitrosamines are more readily cleaved than those in unconstrained aliphatic *N*-nitrosamines,[29,30,35] and this is the likely reason that we observe the formation of the (por)Fe(NO) products during the room temperature reactions of the aromatic nitrosamines with the four-coordinate (por)Fe^{II} compounds. In contrast, the (por)Fe(NO) compounds do not form readily during the room temperature reactions using the aliphatic nitrosamines.

This denitrosation process is not inconsistent with the observation of P450-dependent denitrosations of nitrosamines,[36] although the direct *N*-binding of nitrosamines to the iron centers in P450 enzymes has not been firmly established to date. We note that a variety of organic nitroso compounds such as alkyl nitrites (RONO), alkyl thionitrites (RSNO), and other *N*-nitroso compounds such as Diazald and NONOates also serve as nitrosylating agents to metal-containing precursors to generate metal-NO moieties.[37−40]

Ferrous Nitrosyl Nitrosamine Derivatives. Adduct formation between ferric porphyrins and NO give the ferric-NO adducts that are best described as $\{FeNO\}^6$ species according to the Enemark-Feltham notation.[41−43] Lehnert and co-workers have recently provided computational and experimental data that illustrated the interesting complexity of the $\{FeNO\}^6$ class of compounds.[44] In some cases, but not in all cases, these ferric-NO moieties may be described as "ferrous-nitrosonium" $Fe^{II}-NO^+$ species.

We explored the possibility that NO may displace one of the nitrosamines in the ferric bis-nitrosamine complexes to form the mixed nitrosyl-nitrosamine derivative.

(29) Zhu, X.-Q.; He, J.-Q.; Li, Q.; Xian, M.; Lu, J.; Cheng, J.-P. *J. Org. Chem.* **2000**, *65*, 6729–6735.
(30) Miura, M.; Sakamoto, S.; Yamaguchi, K.; Ohwada, T. *Tetrahedron Lett.* **2000**, *41*, 3637–3641.
(31) Cheng, L.; Richter-Addo, G. B. In *The Porphyrin Handbook*; Guilard, R., Smith, K., Kadish, K. M., Eds.; Academic Press: New York, 2000; Vol. *4* (Biochemistry and Binding: Activation of Small Molecules), pp 219−291.
(32) Mansuy, D.; Battioni, P.; Chottard, J.-C.; Riche, C.; Chiaroni, A. *J. Am. Chem. Soc.* **1983**, *105*, 455–463.
(33) Sohl, C. D.; Lee, J.; Alguindigue, S. S.; Khan, M. A.; Richter-Addo, G. B. *J. Inorg. Biochem.* **2004**, *98*, 1238–1246.
(34) Wang, L.-S.; Chen, L.; Khan, M. A.; Richter-Addo, G. B. *Chem. Commun.* **1996**, 323–324.
(35) Zhu, X.-Q.; Hao, W.-F.; Tang, H.; Wang, C.-H.; Cheng, J.-P. *J. Am. Chem. Soc.* **2005**, *127*, 2696–2708.
(36) Appel, K. E.; Gorsdorf, S.; Scheper, T.; Spiegelhalder, B.; Wiessler, M.; Schoepke, M.; Engeholm, C.; Kramer, R. In *Relevance to Human Cancer of N-Nitroso Compounds, Tobacco Smoke and Mycotoxins*; O'Neill, I. K., Chen, J., Bartsch, H., Eds.; International Agency for Research on Cancer (IARC): Lyon, France, 1991; Vol. *105*, pp 351−357.
(37) Lee, J.; Chen, L.; West, A. H.; Richter-Addo, G. B. *Chem. Rev.* **2002**, *102*, 1019–1065.
(38) Richter-Addo, G. B. *Acc. Chem. Res.* **1999**, *32*, 529–536.
(39) Wang, P. G.; Xian, M.; Tang, X.; Wu, X.; Wen, Z.; Cai, T.; Janczuk, A. *J. Chem. Rev.* **2002**, *102*, 1091–1134.
(40) Melzer, M. M.; Jarchow-Choy, S.; Kogut, E.; Warren, T. H. *Inorg. Chem.* **2008**, *47*, 10187–10189.
(41) Westcott, B. L.; Enemark, J. H. In *Inorganic Electronic Structure and Spectroscopy*; Lever, A. B. P., Solomon, E. I., Eds.; Wiley and Sons: New York, 1999; Vol. *2* (Applications and Case Studies), Chapter 7.
(42) Feltham, R. D.; Enemark, J. H. *Top. Stereochem.* **1981**, *12*, 155–215.
(43) Enemark, J. H.; Feltham, R. D. *Coord. Chem. Rev.* **1974**, *13*, 339–406.
(44) Praneeth, V. K. K.; Paulat, F.; Berto, T. C.; George, S. D.; Nather, C.; Sulok, C. D.; Lehnert, N. *J. Am. Chem. Soc.* **2008**, *130*, 15288–15303.

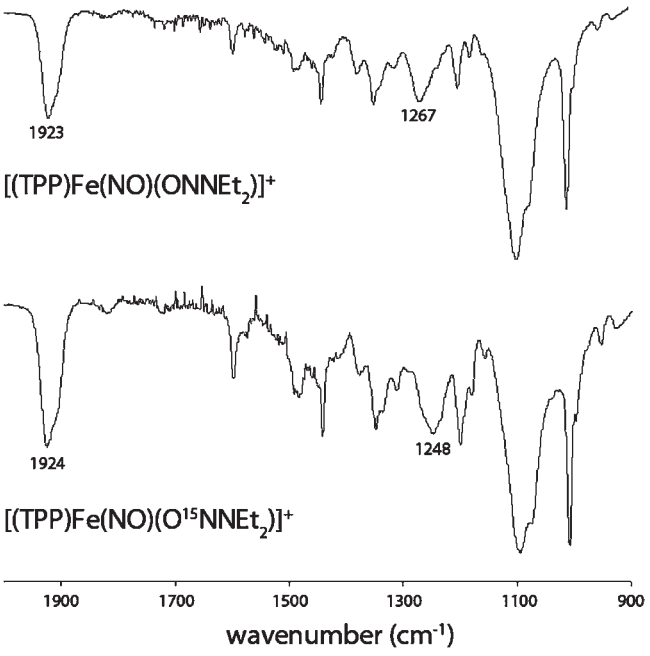

Figure 7. IR spectra of the products from the reactions of the unlabeled and ^{15}N-labeled $[(TPP)Fe(ONNEt_2)_2]ClO_4$ complexes with NO, as dried samples on NaCl plates.

Reaction of ferric $[(TPP)Fe(ONNEt_2)_2]ClO_4$ with NO gas results in the formation of a compound formulated as $[(TPP)Fe(NO)(ONNEt_2)]ClO_4$ based on its IR spectrum (Figure 7).[22]

Thus, a new band at 1923 cm^{-1} becomes apparent in the IR spectrum of the reaction product. This band is assigned to υ_{NO}, whereas the 1267 cm^{-1} band is assigned to the $\upsilon_{NO/NN}$ bands (overlapped) of the coordinated nitrosamine and is shifted by -4 cm^{-1} from the analogous band in its $[(TPP)Fe(ONNEt_2)_2]ClO_4$ precursor (Figure 3, top). The assignment of this band to $\upsilon_{NO/NN}$ is confirmed by ^{15}N-isotope labeling of the nitrosamine (Figure 7, bottom) where the new nitrosamine band at 1248 cm^{-1} is also shifted by -4 cm^{-1} from the analogous band in its $[(TPP)Fe(O^{15}NNEt_2)_2]ClO_4$ precursor (Figure 3, bottom).

Similar IR bands are observed in the spectra of the products from the reactions of NO with $[(TPP)Fe(ONNMe_2)_2]ClO_4$. The product from the reaction of solid $[(TPP)Fe(ONNMe_2)_2]ClO_4$ with NO displays a υ_{NO} at 1910 cm^{-1} with a $\upsilon_{NO/NN}$ that is -3 cm^{-1} shifted upon NO binding. In contrast, the product from the solution phase reaction displays a υ_{NO} at 1922 cm^{-1} and a $\upsilon_{NO/NN}$ that is -11 cm^{-1} shifted upon NO binding. We hypothesize that the product from the solid−gas reaction is probably a kinetic product, and that the product from the solution phase reaction is the thermodynamic product. However, we have yet not been able to crystallize any of these nitrosyl $[(por)Fe(NO)(ONNR_2)]^+$ complexes for a crystal structural determination. Importantly, nitrosyl porphyrins of the $\{FeNO\}^6$ formulation with *trans* water, alcohol, imidazole, indazole, and pyrazine donors display υ_{NO} bands above 1900 cm^{-1}, and these compounds generally contain linear or near-linear FeNO moieties.[31] Thus, the observed υ_{NO}s of the

(45) Rademacher, P.; Stølevik, R. *Acta Chem. Scand.* **1969**, *23*, 660–671.

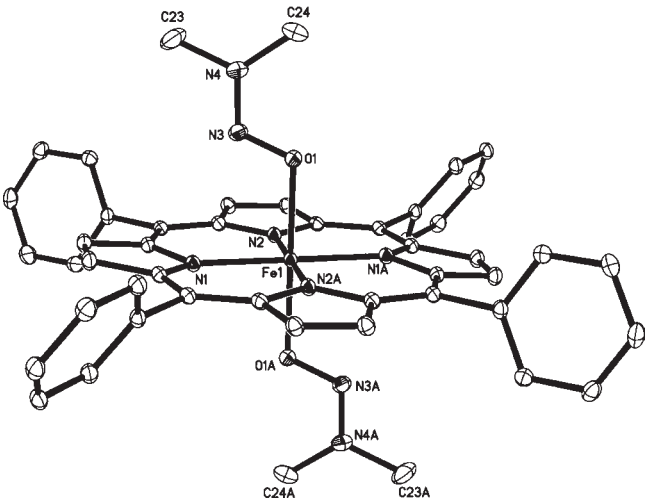

Figure 8. Structure of the cation of $[(TPP)Fe(ONNMe_2)_2]ClO_4$. Hydrogen atoms have been omitted for clarity.

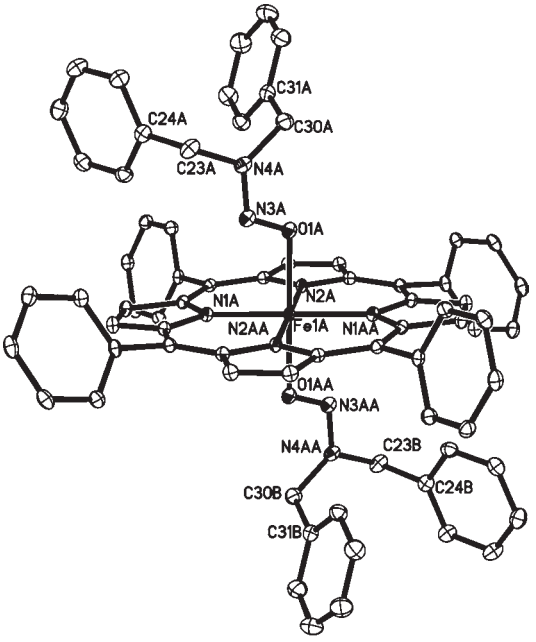

Figure 9. Structure of the cation of $[(TPP)Fe(ONN(CH_2Ph)_2)_2]$-$[(TPP)Fe(OClO_3)_2]$. Hydrogen atoms have been omitted for clarity.

$[(TPP)Fe(NO)(ONNR_2)]ClO_4$ complexes suggest linear or near-linear FeNO geometries in these nitrosyl-nitrosamine complexes. In addition, the similar $\upsilon_{NO/NN}$ band-(s) of the precursor $[(TPP)Fe(ONNR_2)_2]ClO_4$ complexes to those of the nitrosyl derivatives $[(TPP)Fe(NO)$-$(ONNR_2)]ClO_4$ suggest that the nitrosamine *O*-binding mode is retained in the nitrosyl derivatives.

Crystallography and EPR spectroscopy. Bis-nitrosamine Complexes. We were successful in obtaining X-ray diffraction quality crystals of three of the new bis-nitrosamine complexes from their CH_2Cl_2/hexane solutions. The corresponding crystal structures of these compounds

(46) Rademacher, P.; Stølevik, R.; Lüttke, W. *Angew. Chem. Int. Ed. Eng.* **1968**, *7*, 806.

(47) Gdaniec, M.; Milewska, M. J.; Polonski, T. *Angew. Chem., Int. Ed.* **1999**, *38*, 392–395 (CCDC: JOQHEC).

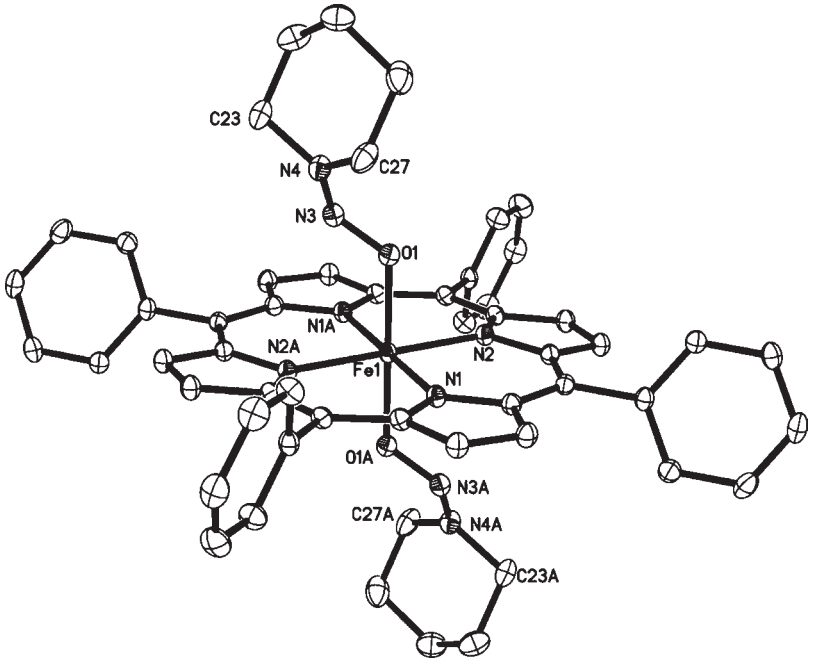

Figure 10. Structure of one of the two independent cations of $[(TPP)Fe(ONN(cyclo\text{-}CH_2)_5)_2]ClO_4$. Hydrogen atoms have been omitted for clarity.

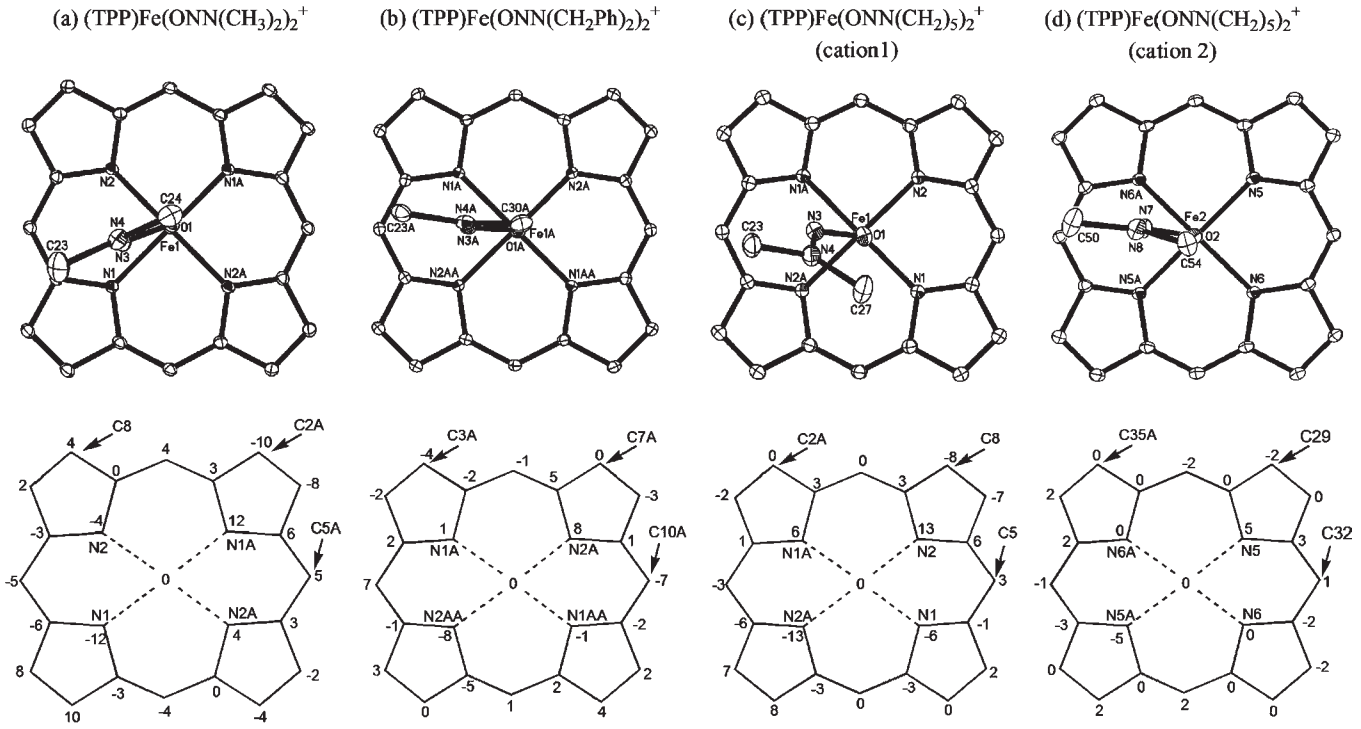

Figure 11. (*Top*) View of the nitrosamine orientations relative to the porphyrin cores, with the view along the axial O−Fe bonds. Nitrosamine substituents have been removed for clarity. (*Bottom*) Perpendicular atom displacements (in units of 0.01 Å) of the porphyrin cores from the 24-atom mean porphyrin planes.

$[(TPP)Fe(ONNMe_2)_2]ClO_4$, $[(TPP)Fe(ONN(CH_2Ph)_2)_2]ClO_4$, and $[(TPP)Fe(ONN(cyclo\text{-}CH_2)_5)_2]ClO_4$ are shown in Figures 8−10, respectively, with a focus on the structures of the nitrosamine-containing cations.

The orientation of the nitrosamine skeletons relative to the respective porphyrin planes are shown in Figure 11, and selected bond lengths and angles are listed in Table 3.

In all three crystal structures, the nitrosamine ligands are O-bound to the ferric centers in these compounds. Prior to this work, the only other structurally characterized iron porphyrin nitrosamine compound was $[(TPP)Fe(ONNEt_2)_2]ClO_4$;[21,22] X-ray structural characterization of this compound also revealed the *O*-binding mode of the diethylnitrosamine ligands. Combined with this latter compound, these remain the only structurally characterized iron porphyrin nitrosamine compounds reported in the literature. Further, these are also the only iron nitrosamine complexes (porphyrin- or

Table 3. Selected Bond Lengths (Å) and Angles (deg) for the Iron Porphyrin Nitrosamine Compounds and Organic Nitrosamines

compound	Fe−O	O−N	N−N	N−C	Fe−N(por)	∠Fe−O−N	∠O−N−N	∠N−N−C	$\angle N_{Tot}$	∠O−Fe−O
$[(OEP)Fe(ONNMe_2)]ClO_4$	2.102(2)	1.251(3)	1.275(3)	1.445(4), 1.465(5)	1.978(2), 1.985(2), 1.985(2), 1.986(2)	109.8(1)	115.9(2)	122.7(3), 116.2(3)	360.0	n.a.
$[(TPP)Fe(ONNMe_2)_2]ClO_4$	2.136(1)	1.271(1)	1.284(1)	1.456(2), 1.458(2)	2.038(1), 2.040(1)	111.5(1)	114.2(1)	122.9(1), 115.6(1)	359.7	180.0
$[(TPP)Fe(ONN(CH_2Ph)_2)_2]$-$[(TPP)Fe(OClO_3)_2]\bullet(CH_2Cl_2)_2$										
cation	2.124(1)	1.271(2)	1.288(2)	1.471(2) 1.469(2)	2.040(1), 2.040(1)	112.7(1)	114.5(1)	124.3(1) 114.3(1)	360.0	180.0(1)
anion	[2.237(1)]				[2.003(1), 1.986(1)]					
$[(TPP)Fe(ONN(c\text{-}CH_2)_5)_2]$-$[ClO_4]\bullet(CH_2Cl_2)_2$										
cation 1	2.086(1)	1.275(2)	1.281(2)	1.465(2) 1.471(3)	2.050(1) 2.046(1)	115.7(1)	114.2(2)	116.7(2) 125.6(2)	359.7	180.0(1)
cation 2	2.110(1)	1.271(2)	1.282(2)	1.462(3) 1.472(3)	2.050(1) 2.042(1)	113.3(1)	114.6(2)	116.6(2) 126.2(2)	359.6	180.0(1)
Me_2NNO[a]		1.235(2)	1.344(2)	1.461(2)			113.6(2)	120.3(3) 116.4(3)		
$(cyclo\text{-}CH_2)_5NNO$[b]		1.252[c]	1.315[c]	1.455[c] 1.442[c]			115.2[c]	117.6[c] 124.6[c]		

[a] Determined by electron diffraction.[45,46] [b] In complex with cholic acid.[47] [c] Data obtained from the Cambridge Structural Database.

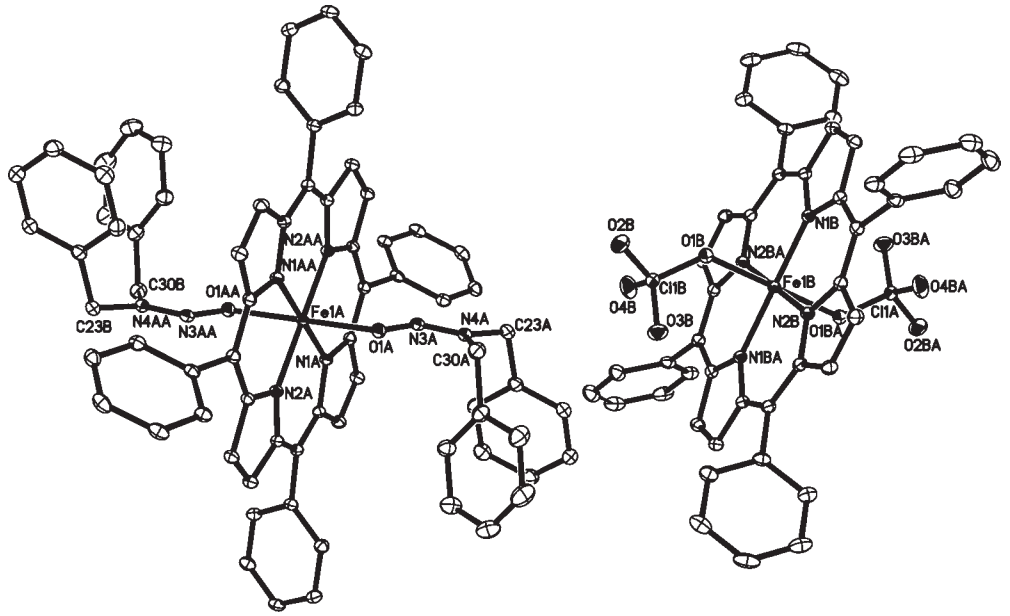

Figure 12. View of the cation and anion of $[(TPP)Fe(ONN(CH_2Ph))_2][(TPP)Fe(OClO_3)_2]$ showing their orientation to each other. Hydrogen atoms have been omitted for clarity.

nonporphyrin-containing) that display the sole *O*-binding mode of the bound nitrosamines (Figure 2c).

That these compounds are best described as having ferric high-spin centers is supported by the analysis of the structural data for the Fe-porphyrin cores,[21,22] and unambiguously by EPR spectroscopy (see later). The equatorial Fe−N(por) and axial Fe−O bond lengths are 2.038(1)−2.050(1) Å and 2.086(1)−2.136(1) Å, respectively; these are similar to the observed data for other high-spin ferric porphyrins as documented by Scheidt and co-workers.[48,49]

(48) Scheidt, W. R.; Reed, C. A. *Chem. Rev.* **1981**, *81*, 543–555.
(49) Scheidt, W. R. In *The Porphyrin Handbook*; Kadish, K. M., Smith, K. M., Guilard, R., Eds.; Academic Press: New York, 2000; Chapter 16.

The crystal structure of $[(TPP)Fe(ONNMe_2)_2]ClO_4$ reveals only one cation (Figure 8) and one associated anion. However, the crystal structure of "$[(TPP)Fe(ONN(CH_2Ph)_2)_2]ClO_4$" reveals the presence of a bis-nitrosamine cation $[(TPP)Fe(ONN(CH_2Ph)_2)_2]^+$ (Figure 9) and a bis-perchlorate anion $[(TPP)Fe(OClO_3)_2]^-$ (Figures 12 and 13). The two porphyrin planes in this $[(TPP)Fe(ONN(PhCH_2)_2)_2][(TPP)Fe(OClO_3)_2]$ complex are oriented 43° to each other (Figure 12). In the porphyrin-containing anion (Figure 13), the Fe−N(por) bonds are 1.986(1)−2.003(1) Å, and the axial Fe−O(ClO_3) bonds are 2.237(1) Å. For comparison, the Fe−N(por) bond distance data for the somewhat related and structurally characterized six-coordinate bis-perchlorate π-cation

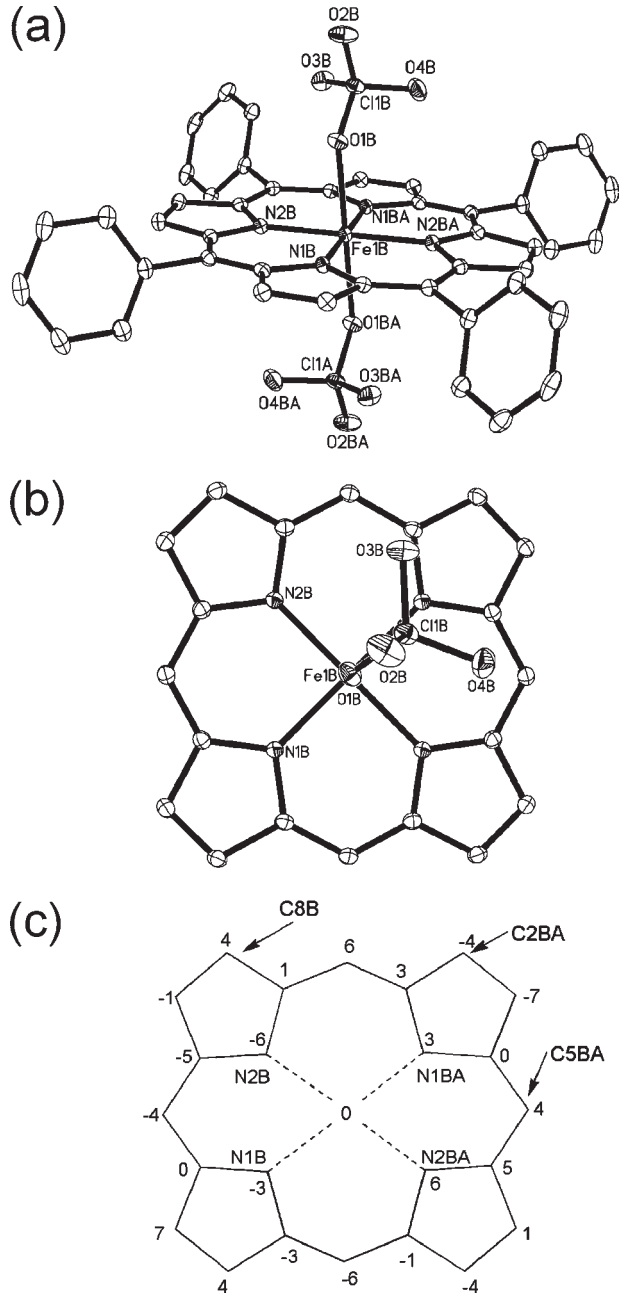

Figure 13. (a) Structure of $[(TPP)Fe(OClO_3)_2]^-$. H atoms have been omitted for clarity. (b) View of the ClO_4^- orientation relative to the porphyrin core, with the view along the O−Fe bond. (c) Perpendicular atom displacements (in units of 0.01 Å) of the porphyrin core from the 24-atom mean porphyrin plane.

radical compounds $[(por\cdot^+)Fe(OClO_3)_2]$ are 2.045 Å (avg) (por = TPP) and 1.999(2) Å (por = OEP).[50,51] The related axial Fe−O(ClO_3) bond distances are 2.13(1) Å (por = TPP) and 2.148(1) Å (por = OEP). When compared with the data for the cationic $[(por\cdot^+)Fe(OClO_3)_2]$ compounds, the longer Fe−O(ClO_3) bond in the anion $[(TPP)Fe(OClO_3)_2]^-$ suggests a weaker interaction between the Fe(por) unit and the perchlorates in this latter electron-rich complex.

To the best of our knowledge, the structure of $[(TPP)Fe(ONN(PhCH_2)_2)_2][(TPP)Fe(OClO_3)_2]$ contains the first structural data for any bis-perchlorate ferric porphyrin anion (Figures 12 and 13). As shown in Figure 13, the perchlorate ligands essentially eclipse and straddle a porphyrin pyrrole N-atom.

The crystal structure of $[(TPP)Fe(ONN(cyclo\text{-}CH_2)_5)_2]ClO_4$ reveals the presence of two independent cations, and their relative orientations with respect to the perchlorate anion is displayed in Figure 14; the two porphyrin planes are oriented 50° to each other.

Nitrosamine Ligands. In the six-coordinate compounds, the O−N and N−N bond distances are 1.271(2)−1.275(2) Å and 1.281(2)−1.288(2) Å, respectively. The related distances in free Me_2NNO are 1.235(2) Å (O−N) and 1.344(2) Å (N−N) as determined by electron diffraction,[45] and in cocrystallized *N*-nitrosopiperidine are 1.252 Å (O−N) and 1.315 Å (N−N) (Table 3).[47] Thus, the N−O bond distances are longer and N−N bond distances are shorter in the nitrosamine porphyrin complexes, suggesting that the complexed nitrosamines are best represented by a resonance hybrid having a significant contribution from the dipolar structure (Figure 4B) which is also supported by IR spectroscopic data described in the previous sections. The crystal structure of free *N*-nitrosodibenzylamine has not been reported.

In all the bis-nitrosamine porphyrin crystal structures, the sums of angles around the amino N-atoms of the bound nitrosamines are 360°, consistent with a significant contribution of the dipolar resonance structure shown in Figure 4B that necessitate planarity of this amino N-atom. In addition, in the $[(TPP)Fe(ONNMe_2)_2]^+$ cation (Figure 8), the nitrosamine atoms O1, N3, N4, C23, and C24 are essentially in a planar arrangement, with O1−N3−N4−C23 and O1−N3−N4−C24 torsion angles of −175.0° and −0.8°, respectively, with a mean deviation of 0.02 Å from the $ONNC_2$ plane. A similar planarity of the five atoms ($ONNC_2$) is observed in $[(TPP)Fe(ONN(CH_2Ph)_2)_2]^+$ and $[(TPP)Fe(ONN(cyclo\text{-}CH_2)_5)_2]^+$ which is consistent with the significant contribution from the dipolar structures in these coordinated nitrosamines. The deviations of the nitrosamine N−N bonds from the normal to the porphyrin planes are 6.0° (for the Me_2NNO complex; Figure 11a) and 1.8° (for the $(PhCH_2)_2NNO$ complex; Figure 11b), revealing the near perpendicularity of the nitrosamine planes to the porphyrin planes in these two complexes. In the $(cyclo\text{-}CH_2)_5NNO$ complex, however, which contains two independent cations, the corresponding deviations of the nitrosamine N−N bonds from the normal to the porphyrin planes are 32.5° (for cation 1; Figure 11c) and 4.5° (cation 2; Figure 11d). The deviation from perpendicularity is evident in the comparison of Figures 11c and 11d. The off-axis tilts (from the porphyrin normal) of the axial Fe−O bonds are 2.8° (for the Me_2NNO complex) and 3.7° (for the $(PhCH_2)_2NNO$ complex). The data for the two cations of the $((cyclo\text{-}CH_2)_5)_2NNO$ complex are 9.3° (cation 1) and 3.0° (cation 2). Clearly, cation 1 of this latter complex displays the largest deviations from perpendicular binding of the nitrosamine ligands to the iron center.

Interestingly, the two internal N−N−R angles in the bound nitrosamines are not equivalent. The internal

(50) Scheidt, W. R.; Song, H. S.; Haller, K. J.; Safo, M. K.; Orosz, R. D.; Reed, C. A.; Debrunner, P. G.; Schulz, C. E. *Inorg. Chem.* **1992**, *31*, 939–941.

(51) Gans, P.; Buisson, G.; Duee, E.; Marchon, J. C.; Erler, B. S.; Scholz, W. F.; Reed, C. A. *J. Am. Chem. Soc.* **1986**, *108*, 1223–1234.

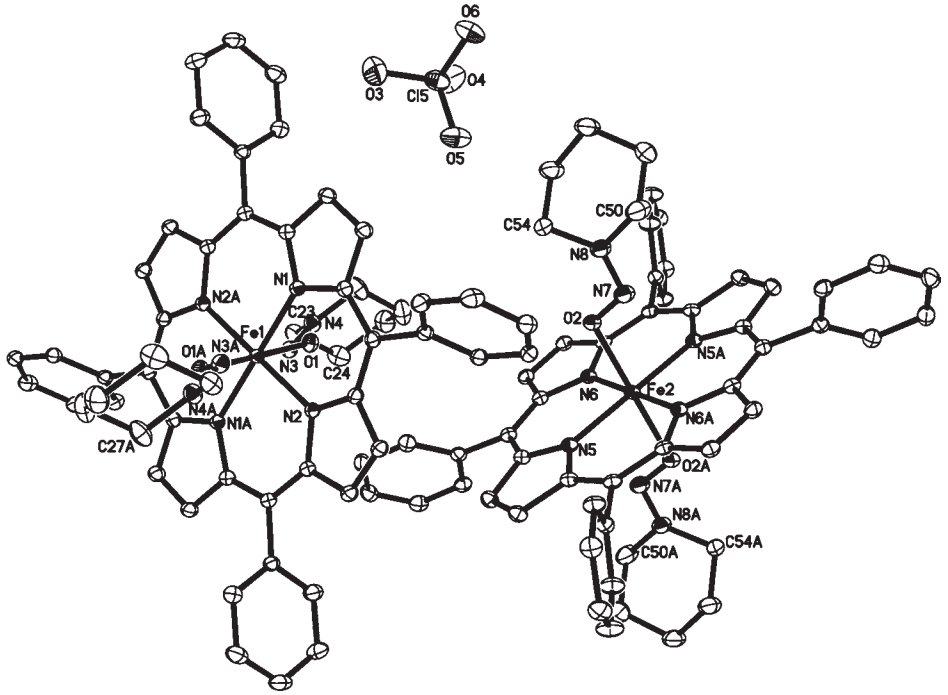

Figure 14. View of the two cations of $[(TPP)Fe(ONN(cyclo\text{-}CH_2)_5)_2]ClO_4$ showing their orientation with respect to the perchlorate anion.

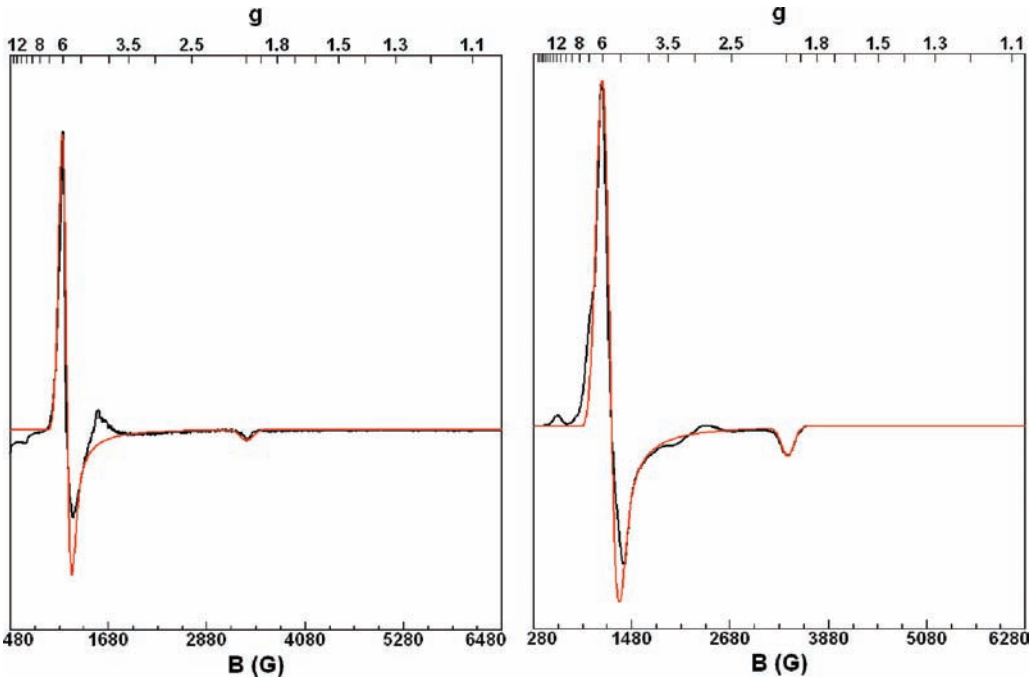

Figure 15. (*Left*) 5 K solution EPR spectrum (black) of 3 mM $[(TPP)Fe(ONNMe_2)_2]ClO_4$ in toluene in the presence of 200 equiv of *N*-nitrosodimethylamine, and simulated spectrum (red). Fit parameters: $S = 5/2$; $D = 10\ cm^{-1}$, $E/D = 0.020$; $g_x = 2.050$, $g_y = 1.950$, $g_z = 2.010$; 9.429 GHz. (*Right*) 5 K solid-state EPR spectrum of $[(TPP)Fe(ONNMe_2)_2]ClO_4$ (black) and simulated spectrum (red). Fit parameters: $S = 5/2$; $D = 10\ cm^{-1}$, $E/D = 0.025$; $g_x = 1.950$, $g_y = 1.950$, $g_z = 2.010$; 9.424 GHz. (See also Table 4).

angle, labeled as ***L*** below, is consistently larger than the outer angle labeled as ***S***.

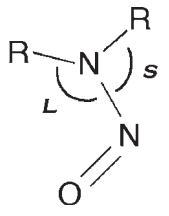

Thus, the internal angles range from 114.27(12)−116.67(16)°, and the outer angles range from 122.86(11)−126.17(17)°. We are currently not able to provide an explanation for this variation, as there does not appear to be any steric reasons (e.g., from steric clashes) for this difference.

We recorded and analyzed the low-temperature frozen-solution and solid-state EPR spectra of the complex $[(TPP)Fe(ONNMe_2)_2]ClO_4$ to unambiguously determine

Table 4. Fit Parameters for the EPR Spectra of Ferric Porphyrin Nitrosamine Compounds, Recorded at 5 K

compound	rel. ratio	S	D (cm^{-1})	E/D	J (cm^{-1})	g_x	g_y	g_z	Δg_x[a]	Δg_y[a]	Δg_z[a]
$[(TPP)Fe(ONNMe_2)_2]ClO_4$											
solution		5/2	10	0.020		2.050	1.950	2.010	0.080	0.080	0.045
solid		5/2	10	0.025		1.950	1.950	2.010	0.130	0.110	0.049
$[(OEP)Fe(ONNMe_2)]ClO_4$											
blue trace[b]	1.00	3/2	10	0.030	2.0	2.070	2.070	2.070	0.370	0.370	0.600
red trace[b]	0.002	3/2	10	0.030	0.7	2.000	2.150	2.150	0.300	0.070	0.070
black trace[b]	0.0001	5/2	10	0.010		1.952	1.950	2.010	0.080	0.080	0.013

[a] Δg is the g strain. [b] The individual components are represented as color traces in Figure 19.

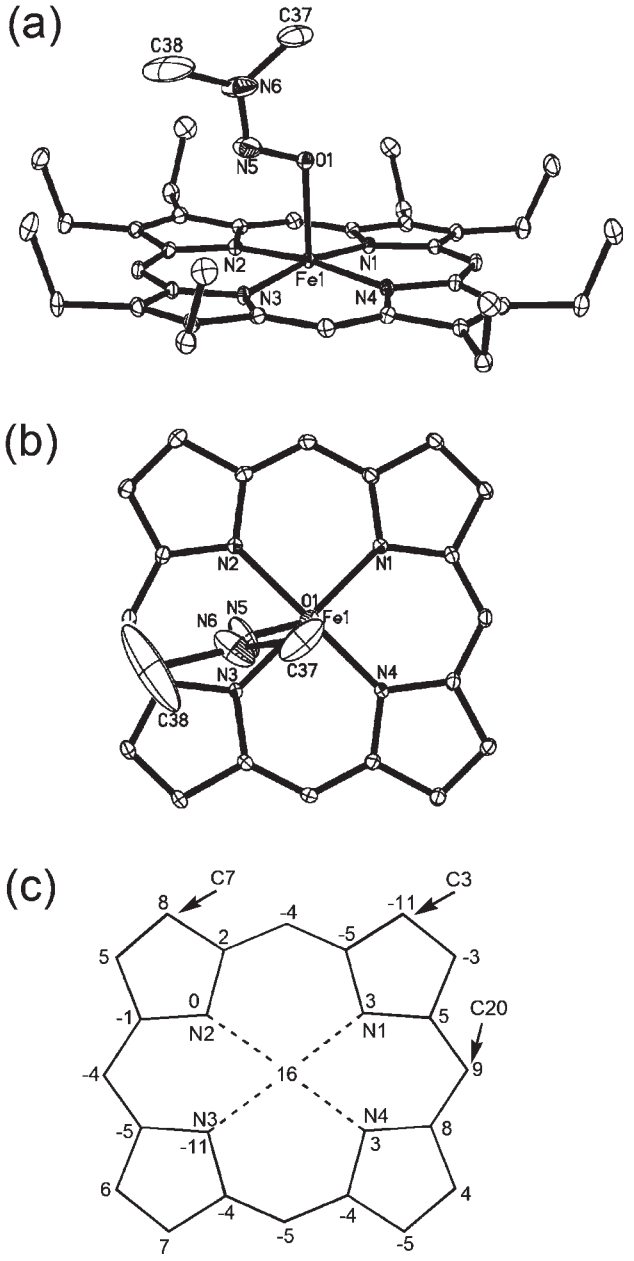

Figure 16. (a) Structure of the cation of $[(OEP)Fe(ONNMe_2)]ClO_4$. Hydrogen atoms have been omitted for clarity. (b) View of the Me_2NNO orientation relative to the porphyrin core, with the view along the O−Fe bond. (c) Perpendicular atom displacements (in units of 0.01 Å) of the porphyrin core from the 24-atom mean porphyrin plane.

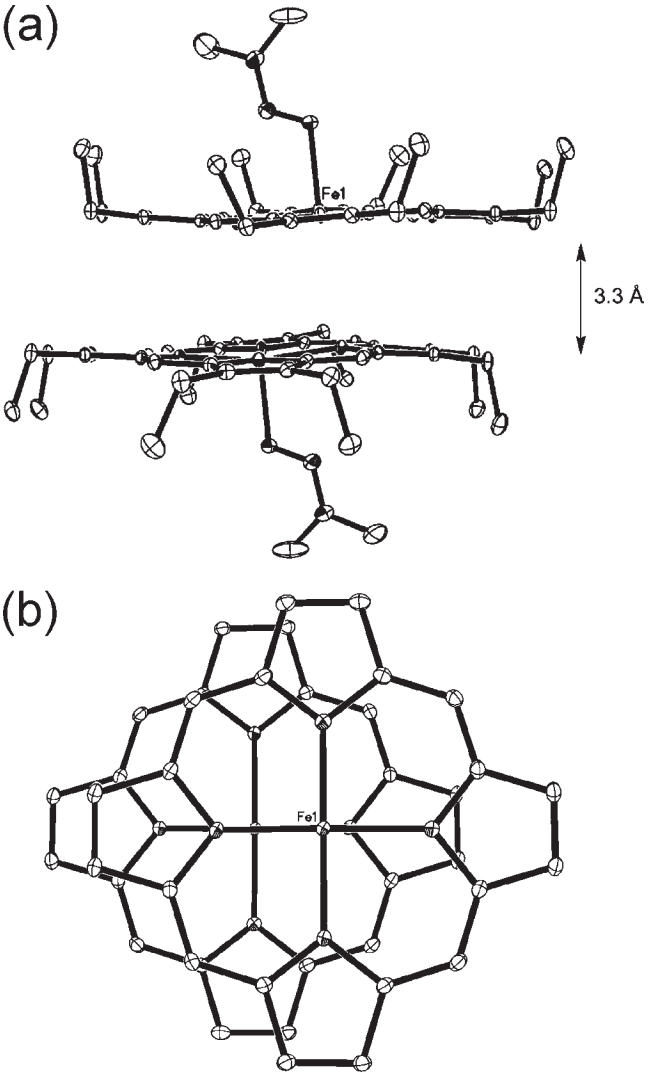

Figure 17. View of the $\pi-\pi$ stacking involving the cation of $[(OEP)Fe(ONNMe_2)]ClO_4$, showing (top) the 3.3 Å separation of the porphyrin planes, and (b) the slippage of the porphyrin rings relative to each other. Hydrogen atoms have been omitted for clarity.

the spin-state of the metal center. The EPR spectrum of the complex in toluene at 5 K is shown on the left of Figure 15 (experimental trace in black, and simulated trace in red), and the spectrum of the complex as a solid (also at 5 K) is shown on the right. Displaying effective g values of ~6 and 2, the data clearly point to a six-coordinate high-spin ferric metal center with a spin of $S = 5/2$ in an effectively axial ligand field ($E/D \sim 0.02$). The magnitude of the D value is not well defined in the simulation, but is clearly $> 5\ cm^{-1}$. The high-spin state is commonly observed for six-coordinate ferric porphyrins

(52) Hoshino, A.; Ohgo, Y.; Nakamura, M. *Inorg. Chem.* **2005**, *44*, 7333–7344.

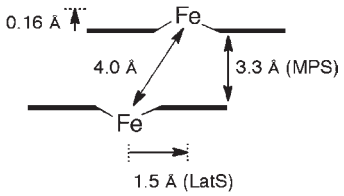

Figure 18. Sketch of the geometric parameters for the OEP-OEP π stacking.

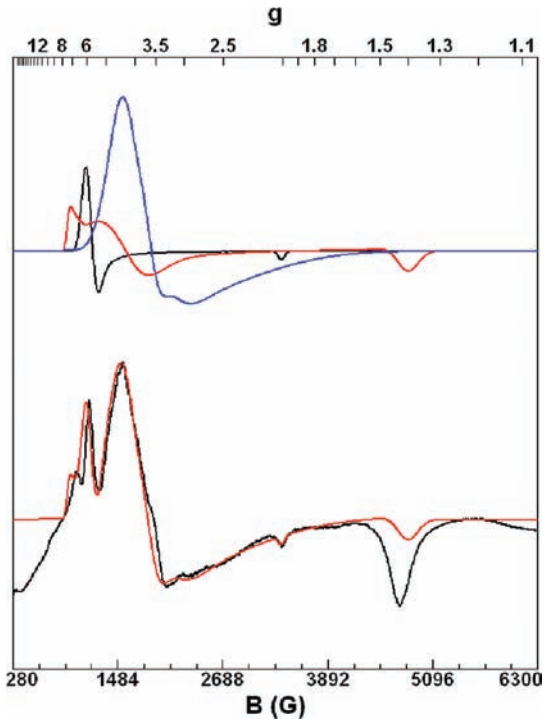

Figure 19. (*Bottom*) 5 K solid-state EPR spectrum of [(OEP)Fe(ONNMe$_2$)]ClO$_4$ (black line) and the simulated spectrum (red line) based on the sum of the spectra of three different species as shown on the top. (*Top*) Simulation of three individual species present in the solid-state EPR spectrum of [(OEP)Fe(ONNMe$_2$)]ClO$_4$. The ratio of the three species blue/red/black is 1:0.002:0.0001. Fit parameters (9.424 GHz): Blue: $S = 3/2$; $D = 10\ \text{cm}^{-1}$, $E/D = 0.030$; $J = 2.0\ \text{cm}^{-1}$; $g_x = 2.070$, $g_y = 2.070$, $g_z = 2.070$; Red: $S = 3/2$; $D = 10\ \text{cm}^{-1}$, $E/D = 0.030$; $J = 0.7\ \text{cm}^{-1}$; $g_x = 2.000$, $g_y = 2.150$, $g_z = 2.150$; Black: $S = 5/2$; $D = 10\ \text{cm}^{-1}$, $E/D = 0.010$; $g_x = 1.952$, $g_y = 1.950$, $g_z = 2.010$. All fit parameters are listed in Table 4.

with weak O-bonded ligands, such as pyridine-*N*-oxide, DMSO, DMF, and MeOH.[52,53] All EPR fit parameters are listed in Table 4.

Five-Coordinate Complex. We were fortunate, using a combination of an octaethylporphyrin macrocycle and dimethylnitrosamine, to achieve the crystallization of a five-coordinate iron porphyrin nitrosamine complex [(OEP)Fe(ONNMe$_2$)]ClO$_4$. The structure of the cation and the axial (perpendicular) orientation of the nitrosamine relative to the porphyrin plane is shown in Figure 16. There are several points to note about this structure. The Fe atom is axially displaced from the 24-atom mean porphyrin plane by 0.16 Å toward the nitrosamine ligand. Such axial displacements of Fe from the mean porphyrin planes in five-coordinate iron porphyrins is not uncommon. Interestingly, however, the geometrical data for the bound nitrosamine in this five-coordinate complex reveals significant differences when compared with the data from the six-coordinate analogues. For example, the O−N bond distance is 1.251(3) Å, which is significantly shorter than the ~1.27 Å distances in the related six-coordinate complexes. This is probably due to a decreased dipolar resonance contribution (**B** in Figure 4) in the stabilization of the nitrosamine coordination to the more electron-rich OEP complex. However, the N−N bond distance of 1.275(3) Å is not significantly different from the analogous distances in the six-coordinate derivatives. The Fe−O−N bond angle of 109.8(1)° in this five-coordinate compound is smaller than the related angles in the six-coordinate complexes, and the tilt of the Fe−O vector from the normal to the porphyrin plane is 4.5°.

The [(OEP)Fe(ONNMe$_2$)]ClO$_4$ complex has a "dimeric" nature involving $\pi-\pi$ stacking interactions between the OEP macrocycles (Figure 17a). This is possible because the π systems of the porphyrin rings effectively block the sixth coordination site and provide additional stabilization of the five-coordinate complex during its crystallization. The mean plane separation (M.P.S.) between the 24-atom porphyrin planes is 3.3 Å, and the Fe−Fe distance is 3.9 Å (Figure 18). The lateral shift, defined here as the "apparent horizontal slippage of one porphyrin with respect to the other" is ~1.5 Å; this horizontal slippage is illustrated in Figure 17b. This $\pi-\pi$ stacking interaction, combined with the magnitudes of the MPS and the lateral shift, places this compound in Class S with a strong $\pi-\pi$ interaction, according to the nomenclature of Scheidt and Lee[54] and in the same group as the [(OEP)Fe(NO)]$^+$ compound.[55] This strong $\pi-\pi$ interaction, when combined with the shorter observed Fe−N(por) distances of ~1.98 Å (cf. 2.04−2.05 Å in the six-coordinate high-spin derivatives discussed above) suggests a different spin-state for this five-coordinate ferric compound.

The experimental solid-state EPR spectrum of [(OEP)Fe(ONNMe$_2$)]ClO$_4$ at 5 K (Figure 19, bottom (black line)) reveals a more complicated situation than the six-coordinate ferric nitrosoamine compounds described above. In this case, the main signal is centered around an effective g value of 3.5 as shown in Figure 19, bottom, which corresponds to an intermediate-spin ($S = 3/2$) complex. Simulation of the experimental spectrum (Figure 19, top) suggests the presence of three species in a 1.00:0.002:0.0001 ratio. These species have been identified as

(i) a largely predominant intermediate-spin species displaying relatively weak exchange coupling of two Fe centers ($S = 3/2$; $J = 2\ \text{cm}^{-1}$; using the Spin Hamiltonian $\underline{\boldsymbol{H}} = J_{\text{AB}}\cdot\underline{\boldsymbol{S}}_{\text{A}}\cdot\underline{\boldsymbol{S}}_{\text{B}}$) in the face-to-face arrangement of two complexes as determined from the crystal structure. The antiferromagnetic exchange coupling with $J = 2\ \text{cm}^{-1}$ is necessary to fit the shape of the $g \sim 3.5$ feature. As before, the value of D is not well-defined, but D is clearly $> 5\ \text{cm}^{-1}$;

(53) Mashiko, T.; Kastner, M. E.; Spartalian, K.; Scheidt, W. R.; Reed, C. A. *J. Am. Chem. Soc.* **1978**, *100*, 6354–6362.

(54) Scheidt, W. R.; Lee, Y. J. *Struct. Bonding* (*Berlin*) **1987**, *64*, 1–70.

(55) Ellison, M. K.; Schulz, C. E.; Scheidt, W. R. *Inorg. Chem.* **2000**, *39*, 5102–5110.

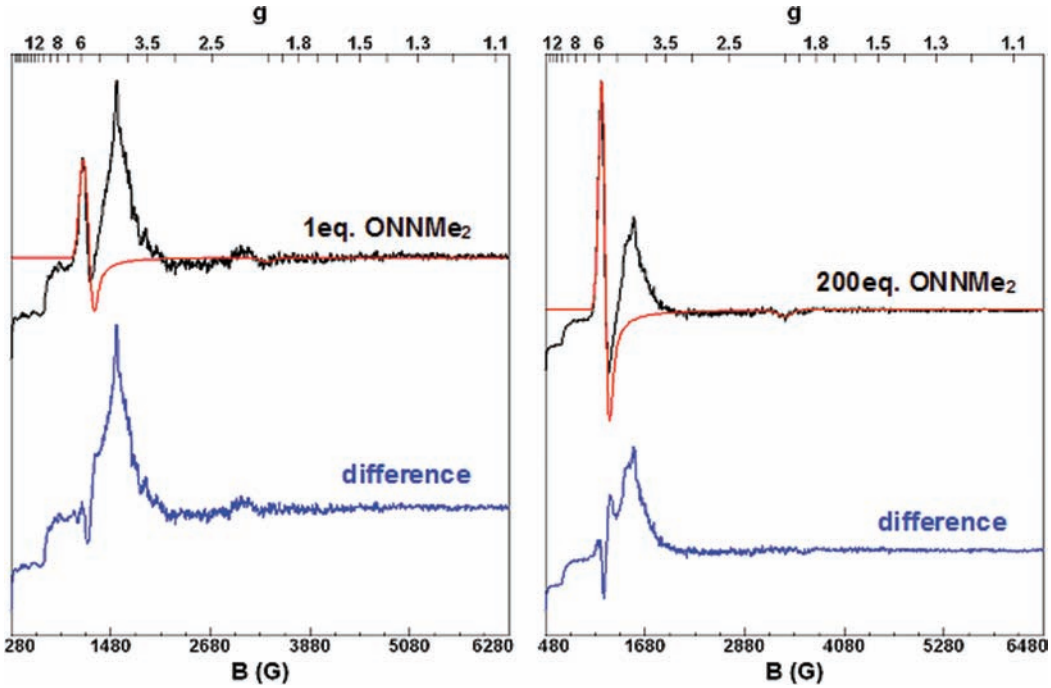

Figure 20. (*Left*) 5 K frozen-solution EPR spectrum of 3 mM $[(OEP)Fe(ONNMe_2)]ClO_4$ in toluene with 1 equiv of Me_2NNO present (top, black trace). The red trace shows the simulated spectrum of the six-coordinate high-spin ($S = 5/2$) complex, and the final difference spectrum (black−red) is shown in blue in the bottom panel. (*Right*) 5 K frozen-solution EPR spectrum of 3 mM $[(OEP)Fe(ONNMe_2)]ClO_4$ in toluene in the presence of 200 equiv of Me_2NNO (black trace, top). The red trace shows the simulated spectrum of the six-coordinate high-spin ($S = 5/2$) complex, and the final difference spectrum (black−red) is shown in blue in the bottom panel. In both cases, the signal of the six-coordinate high-spin ($S = 5/2$) bis-nitrosamine complex does not completely cancel out in the difference spectrum (blue traces) because the simulation does not fully reproduce the experimental shape of the frozen-solution EPR spectrum of the high-spin species as evident from Figure 15, left.

(ii) a second intermediate-spin species (impurity) with a weaker coupling between two Fe centers ($S = 3/2$; $J = 0.7\ cm^{-1}$). Here, the weaker antiferromagnetic coupling of $J = 0.7\ cm^{-1}$ is necessary to fit the signal at $g \sim 1.4$; and

(iii) a very small amount of an impurity, likely of the six-coordinate high-spin ($S = 5/2$) complex with two nitrosamines bound to the ferric heme.

EPR spectroscopy on frozen solutions of the five-coordinate complex $[(OEP)Fe(ONNMe_2)]ClO_4$ at 5 K in toluene further suggests that in the presence of excess ligand, this compound converts to the corresponding bis-ligated six-coordinate species. The frozen-solution EPR spectrum of $[(OEP)Fe(ONNMe_2)]ClO_4$ in the presence of an additional small amount (1 equiv) of ligand is shown in Figure 20, left (black line), and reveals that the predominant species is the five-coordinate intermediate-spin complex with only a small amount of the six-coordinate species present. Addition of excess ligand then leads to the conversion of the magnitude of the five-coordinate complex to the six-coordinate high-spin derivative $[(OEP)Fe(ONNMe_2)_2]ClO_4$ as shown in Figure 20, right. As expected, the strong signal at $g \sim 1.4$ observed in the solid state is missing in the solution data, again emphasizing that this signal is likely due to weak antiferromagnetic exchange coupling between two complexes in the face-to-face arrangement observed in the crystal structure (Figure 17a). This signal therefore disappears in the solution spectra.

Summary

We have prepared a number of nitrosamine adducts of synthetic iron porphyrins from the reactions of the cationic $[(por)Fe(THF)_2]ClO_4$ precursors in toluene with dialkylnitrosamines. We have structurally characterized, by single-crystal X-ray crystallography, three six-coordinate $[(por)Fe(ONNR_2)_2]ClO_4$ compounds and a five-coordinate $[(OEP)Fe(ONNMe_2)]ClO_4$ derivative. We have shown that the N−O and N−N vibrations of the coordinated nitrosamine groups in the $[(por)Fe(ONNR_2)_2]ClO_4$ complexes occur in the 1239−1271 cm^{-1} range. EPR spectroscopy at liquid He temperature reveals a high-spin ferric center in the six-coordinate bis-nitrosamine $[(TPP)Fe(ONNMe_2)_2]ClO_4$ complex, but an intermediate-spin ferric center in the five-coordinate mononitrosamine $[(OEP)Fe(ONNMe_2)]ClO_4$ derivative. Importantly, all the nitrosamine ligands in the complexes reported here bind to the ferric centers via a sole η^1-O binding mode. This class of compounds represents the only reported examples of isolable iron porphyrins complexed with nitrosamine ligands. Given the observation that nitrosamines can bind directly to the ferric center in P450 enzymes, we can conclude that the observed O-binding of nitrosamines in our ferric model systems is possible for ferric P450s as well. Such binding may, by itself, not lead directly to metabolic reactivity of the nitrosamines. On the other hand, the ferrous derivatives are more prone to display chemical reactivity of the bound nitrosamines.

Acknowledgment. We are grateful to the National Institutes of Health (GM-064476; G.B.R.A.) and the National Science Foundation (CHE-0846235; N.L.) for

funding of this research. The authors thank the National Science Foundation (CHE-0130835; G.B.R.A.) and the University of Oklahoma for funds to purchase of the X-ray diffractometer and computers.

Supporting Information Available: Figures S1−S15 containing IR spectra. This material is available free of charge via the Internet at http://pubs.acs.org. CCDC 745891−745894 contains the supplementary crystallographic data for this paper. These data can be obtained free of charge via www.ccdc.cam.ac.uk/data_request/cif, or by emailing data_request@ccdc.cam.ac.uk, or by contacting The Cambridge Crystallographic Data Centre, 12, Union Road, Cambridge CB2 1EZ, U.K.; fax: +44 1223 336033.